CHALMERS
UNIVERSITY OF TECHNOLOGY

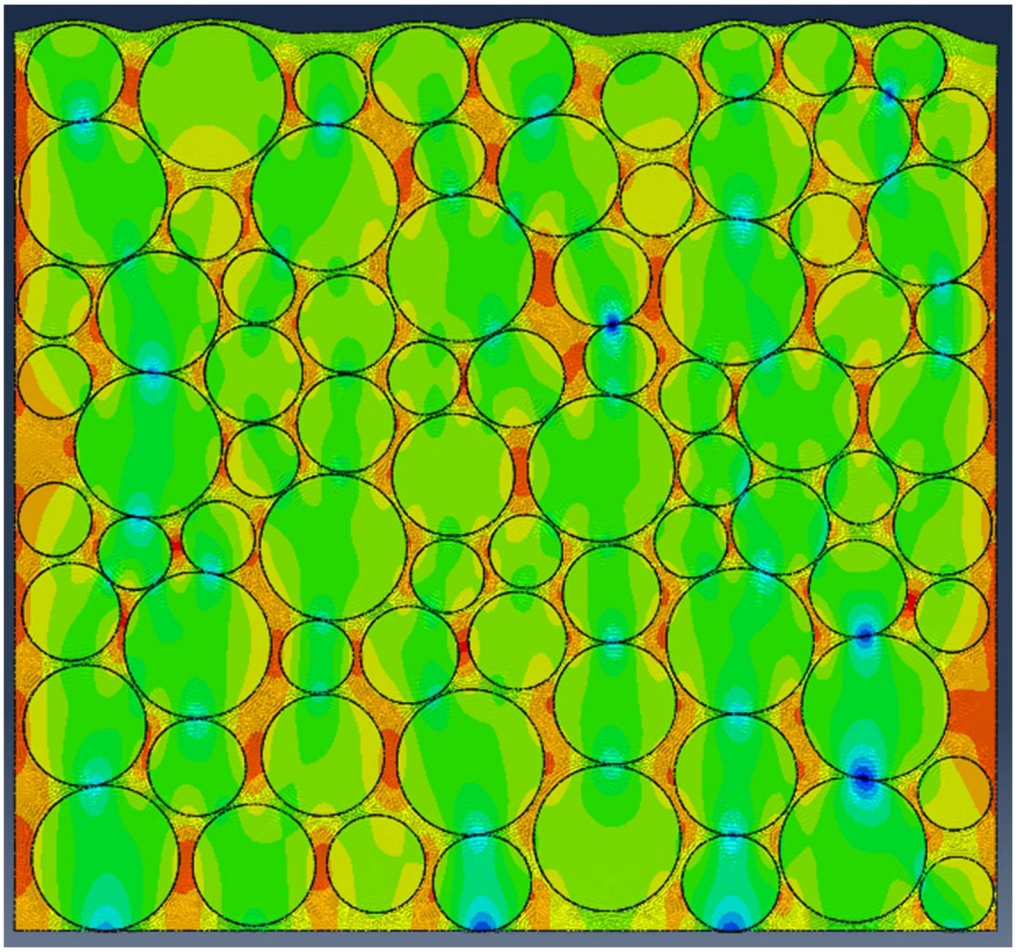

Structural Investigation of an Alternative Cordwood Binder

Master's thesis in the Master's Programme Structural Engineering and Building Technology

OLOF STÅLHAMMAR

DEPARTMENT OF ARCHITECTURE AND CIVIL ENGINEERING

CHALMERS UNIVERSITY OF TECHNOLOGY
Gothenburg, Sweden 2026
www.chalmers.se

MASTER'S THESIS ACEX30

Structural Investigation of an Alternative Cordwood Binder

Master's Thesis in the Master's Programme Structural Engineering and Building Technology

OLOF STÅLHAMMAR

Department of Architecture and Civil Engineering
Division of Building Technology
Arezou Ahmadi
Yutaka Goto
CHALMERS UNIVERSITY OF TECHNOLOGY
Göteborg, Sweden 2026

Structural Investigation of an Alternative Cordwood Binder

Master's Thesis in the Master's Programme Structural Engineering and Building Technology

OLOF STÅLHAMMAR

Examensarbete ACEX30
Institutionen för arkitektur och samhällsbyggnadsteknik
Chalmers tekniska högskola, 2026

Department of Architecture and Civil Engineering
Division of Building Technology
Chalmers University of Technology
SE-412 96 Göteborg
Sweden
Telephone: + 46 (0)31-772 1000

Cover:
Absolute stresses in a cordwood wall using a lignin binder
Department of Architecture and Civil Engineering
Göteborg, Sweden, 2026

Structural Investigation of Alternative Cordwood Binder

Master's thesis in the Master's Programme Structural Engineering and Building Technology

OLOF STÅLHAMMAR

Department of Architecture and Civil Engineering
Division of Building Technology
Chalmers University of Technology

ABSTRACT

Cordwood masonry is a vernacular building technique that utilizes short pieces of wood in a binder matrix. The binder matrix used today is usually cement, lime-mortar or clay all with various downsides including thermal bridging, high environmental impact or difficulties of separating the materials at end of life. A novel binder made of a mixture of starch-based glue, lignin and saw dust is investigated to determine if the mechanical properties make it suitable to serve as an alternative. Samples of the binder are tested experimentally to find how it reacts to an outdoor environment and compressive strength. The parameters are used to develop a model of a wall element for FE-analysis that is compared with calculations based on Eurocode to verify the suitability of the material.

This thesis found the best binder candidate to be one with two parts lignin and one part saw dust. This binder has a compressive strength of 0.4 N/mm^2 and a modulus of elasticity of 13.7 N/mm^2. This is sufficient for walls in a one-story building according to both the Eurocode calculations and the FE-model. This binder candidate withstood the weather during the three-month trial with only little damage while other candidates partially dissolved after 30-40 days in an exposed environment. The binder performed even better in a semi-sheltered environment, with little to no visible damage.

Key words: Cordwood masonry, finite element modelling, lignin, compression test, binder

Strukturell utforskning av alternativa bindemedel för vedmurning

Examensarbete inom masterprogrammet Master' Konstruktionsteknik och byggnadsteknologi

OLOF STÅLHAMMAR

Institutionen för arkitektur och samhällsbyggnadsteknik

Avdelningen för Byggnadsteknologi

Chalmers tekniska högskola

SAMMANFATTNING

Kubbhus eller vedmurning är en vernakulär byggteknik som använder korta vedträd i en matris av murbruk. Den murbruken som används idag är vanligtvis cement, kalkmurbruk eller lera, alla med olika nackdelar, inklusive köldbryggor, hög miljöpåverkan eller svårigheter att separera materialen vid slutet av livscykeln. Ett nytt bindemedel tillverkat av en blandning av stärkelsebaserat lim, lignin och sågspån undersöks i den här rapporten för att avgöra om de mekaniska egenskaperna gör det lämpligt att fungera som ett alternativ. Prover av bindemedlet testas experimentellt för att hitta miljöstabilitet och tryckhållfasthet. Parametrarna används för att utveckla en modell av ett väggelement för FE-analys som jämförs med beräkningar baserade på Eurocode för att verifiera materialets lämplighet.

Denna mastersuppsats fann att den bästa bindemedelskandidaten var ett med två delar lignin och en del sågspån. Detta bindemedel har en tryckhållfasthet på 0,4 N/mm^2 och en elasticitetsmodul på 13,7 N/mm^2. Detta är tillräckligt för väggar i en envåningsbyggnad enligt både Eurocode-beräkningarna och FE-modellen. Denna bindemedelskandidat klarade vädret under den tre månader långa försöksperioden med endast liten skada, medan andra kandidater delvis upplöstes efter 30–40 dagar i en exponerad miljö. Bindemedlet presterade ännu bättre i en halvskyddad miljö, med liten eller ingen synlig skada.

Nyckelord: Kubbhus, vedmureri, finita-elementmetoden, lignin, tryckhållfasthetstest, bindemedel

Contents

1 Contents

Preface

This thesis started as a continuation of my Master's Thesis in Architecture: *Globwood - Cellulose-Glue Binder For Cordwood Masonry* which explored the architectural implications of cordwood construction while introducing the topic of lignin-based binders. This work focuses on the binders introduced in that thesis and performs test that were beyond the scope of an architectural thesis.

Both works own thanks to the experimental work with light weight binders that Olle Hagman performed.

Göteborg May 2026

OLOF STÅLHAMMAR

List of Figures

Figure 4.11:
a) Stålhammar, O. (2026) *Normalized volume over time for SSS specimen while drying for different lengths of wetting.* [graph]
b) Stålhammar, O. (2026) *Normalized volume over time for SSL specimen while drying for different lengths of wetting.* [graph]
c) Stålhammar, O. (2026) *Normalized volume over time for SLL specimen while drying for different lengths of wetting.* [graph]
d) Stålhammar, O. (2026) *Normalized volume over time for LLL specimen while drying for different lengths of wetting.* [graph]

Figure 4.12:
Stålhammar, O. (2026) *Maximum Stress/Time in water Compressive test: Impact of wetting.* [graph]

Figure 5.1:
a) Stålhammar, O. (2025) *Exploded isometry of The Globwood Retreat.* [digital drawing]
b) Stålhammar, O. (2025) *Plan of The Globwood Retreat.* [digital drawing]

Figure 5.2:
a) Stålhammar, O. (2025) *Analysis area for finite-element model.* [digital drawing]
b) Stålhammar, O. (2026) *Formfactor for vaulted roofs.* [digital drawing]
Adapted from Swedish Standards Institute (2005) SS-EN 1991-1-3:2003 *Eurocode 1 – Actions on structures – Part 1-3: General actions – Snow loads.* Stockholm, Swedish Standards Institute. Figure 5.6 *Formfactor for snow load on vaulted roofs*

Figure 5.3:
a) Stålhammar, O. (2026) *Geometry for finite-element model.* [digital]
b) Stålhammar, O. (2026) *Radii of log-ends.* [digital]

Figure 5.4:
a) Stålhammar, O. (2026) *Loads and boundary conditions of finite-element model.* [digital]
b) Stålhammar, O. (2026) *Finite-element model mesh.* [digital]

Figure 6.1:
Stålhammar, O. (2026) *Maximum von Mises stress compared with the number of mesh elements showing convergence.* [digital]

Figure 6.2:
Stålhammar, O. (2026) *Section of FEM geometry at different mesh densities.* [digital]

Figure 6.3:
Stålhammar, O. (2026) *FEA results showing maximum absolute principal stresses of the analysis area using the SLL binder.* [digital]

Figure 6.4:

a) Stålhammar, O. (2026) *FEA results showing maximum absolute principal stresses of the analysis area using a cement binder.* [digital]
b) Stålhammar, O. (2026) *FEA results showing maximum absolute principal stresses of the analysis area using a clay binder.* [digital]

Notations

Roman upper-case letters

Ce	is the exposure factor.
Ct	is the thermal coefficient.
G_k	is the permanent load.
G_{Roof}	is the permanent loads from the roof.
G_{Wall}	is the permanent loads from the wall.
K	is a parameter that is unknown for cordwood but the range for other combinations of binders and masonry units is 0.20 - 0.80
M_{id}	is the design value of the moment at the top or bottom
N_{Ed}	is the design value
N_{id}	is the design value of the vertical load at the top or bottom
N_{Rd}	is the design value of the
U_{FEM}	Utilization rate for FEM simulation.
ULS	Ultimate limit state
SLS	Service limit state
LLL	Binder recipe using three parts lignin, one part paper sludge and one part starch-based glue
SLL	Binder recipe using one part saw dust, two parts lignin, one part paper sludge and one part starch-based glue
SSL	Binder recipe using two parts saw dust, one part lignin, one part paper sludge and one part starch-based glue.
SSS	Binder recipe using three parts saw dust, one part paper sludge and one part starch-based glue
CT:IW	is the compressive test of the specimen impacted by wetting.
CT:US	is the compressive test with unmodified specimen.

Roman lower-case letters

e_{he} is the eccentricity at the top or bottom of the wall, if any, resulting from horizontal loads.

e_i is the eccentricity used

e_{init} is the initial eccentricity with a sign that increases the absolute value of e_i

f_b is the compressive strength of the masonry units.

f_d is the dimensioning strength

f_k is the combined compressive strength of the masonry composite.

f_m is the compressive strength of the mortar.

h is the height

h_{ef} is the clear height of the wall.

$k_{mod,i}$ is the partial coefficient for different climate classes

$l_{f,ef}$ is the difference of the effective span of the floors in meters on both sides of the considered wall.

$l_{f,ef,i,}$ 0.9 $l_{f,I}$ for simply supported floors

$l_{ref.c}$ value depending on the characteristic compressive strength of the masonry f_k, the ratio E/f_k and the thickness of the wall t. See table 2.1.

$l_{ref,t}$ value depending on the characteristic compressive strength of masonry f_k and the thickness of the wall t. See table 2.1.

s_k is the characteristic snow-load

w_{vault} is the width of vault.

Greek lower-case letters

α is a constant related to f_b.

β in equation 1 is a constant related to f_m. in figures 2.2 and 5.2 β represents the angle of the roof.

γ_d is a partial coefficient.

γ_M is a partial coefficient.

ϵ is the strain.

μ_i is the formfactor for snow load.

μ_3 is the formfactor for snow loads on vaulted roofs.

ρ_{pine} is the density of pine.

ρ_{roof} is the density of roof.

ρ_{SLL} is the density of SLL binder.

ρ_{SSL} is the density of SSL binder.

ρ_{wall} is the density of wall.

σ is the stress.

$\sigma_{c,MAX}$ is the maximum compressive stress.

$\sigma_{c,MAX,cement}$ is the maximum compressive stress of cement binder.

$\sigma_{c,MAX,clay}$ is the maximum compressive stress of clay binder.

ϕ_i is the reduction factor for the top and bottom of the wall taking account for eccentricity and slenderness.

ϕ_s is the simplified reduction factor for the top and bottom of the wall taking account for eccentricity and slenderness.

ψ_2 is the frequent value for variable loads.

ψ_1 is the quasi-permanent value for variable loads

.

1 Introduction

1.1 Background

The building and construction industry is responsible for around one third of global greenhouse gas emissions and one third of global energy demand, with steel and cement production contributing an outsized amount (United Nations Environment Programme, 2025). This makes sustainability an important focus for innovation. One approach to a more sustainable building industry is to adapt pre-industrial methods of building and another is the use of alternative building materials. This could involve materials such as rammed earth or mycelium with low embodied carbon dioxide. Other alternatives include the capture of current waste streams, such as plastic fibers out at sea or concrete as filler material in new mortars.

Cordwood masonry is a vernacular building technique where log ends (short pieces of firewood, either split or round, alternatively sawn timber) are placed perpendicular to the wall. This method provides both an opportunity to build with low embodied carbon and to capture otherwise existing waste streams from the paper and pulp industry. The log-ends require minimal processing beyond being sawn to size and the occasional split, resulting in low embodied carbon. In addition, the ability to utilize trees of almost any size and shape allows a cordwood building to be constructed by material that otherwise would have been burnt. (Mouterde, R., et al., 2010). The total consumed energy of a cordwood building is according to Mouterde, R. et al. (2010) lower than that of a double wall timber frame building, with otherwise equivalent specifications, in a temperate climate but has higher energy demands due to lower R-values. The timber frame buildings better R value leads the cordwood building to overtake it in consumed energy after 5 years. According to the same source, a cordwood building always has lower energy consumed than an equivalent concrete building over a 50-year period.

However, cordwood construction is not a universal solution to the environmental problems caused by the building industry. The binders used today vary depending on region, but the three most common are clay or cob, lime mortars, and cement (Roy, R. 2016). The latter two are the most common since they are easy to find and work with but bring with them the problem of a relatively high carbon footprint. Reducing the binder's embodied energy is the biggest opportunity for making cordwood building even more sustainable.

This thesis investigates a new alternative binder for cordwood construction. The usefulness of a lignin binder is based on the arguments that a binder based on waste materials provide a less carbon footprint intensive alternative than traditional binders. This could come with economic benefits as well since lignin is an underutilized resource. At the same time, it could allow for easier continuous bonds with better insulation properties than traditional binders. In addition, a bio-based binder can be sorted at end of life together with the timber masonry units.

As cordwood is only used sparingly today, even a significant technical improvement has a limited impact from a broader perspective. This, however, does not mean that cordwood is not worth studying. The people who practice cordwood building today are usually an environmentally conscious group that likes sharing and cultivating

knowledge which is showcased through the workshop culture and through the reports in continental cordwood conference. This means that improvements easily can propagate through the group.

Some examples of traditional scale cordwood walls are given in *figure 1.1*. These show both a modern example and an example of a cordwood wall that is around 150 years old.

Figure 1.1: *Examples of traditional scale cordwood buildings a) Barn in Hållnäs, Sweden, with walls built using a mix of cement binders and lime binders, the building is around 150 years old b) Cordwood house in Sweden built using a clay binder c) 1:5 scale model of cordwood wall using the lignin binder.*

1.2 Literature studies

Only a handful of studies have been written on cordwood construction and even fewer studying wood masonry using different binders. This limits the literature study to more specific areas of the thesis and general information about cordwood.

The initial databases used to find articles in this report were Google Scholar, Web of Science, Scopus, Access Engineering, Avery and CEDB. Only articles in English and Swedish were used. The subject area was limited to Engineering, Materials Science and Architecture. Additional literature was found through reading the sources of the found articles and through consulting the sources used in the author's previous thesis (Stålhammar, O. 2025).

1.2.1 A brief introduction to cordwood construction

Cordwood masonry is a traditional building technique where log ends are laid perpendicular to the wall. The building technique was introduced in the beginning of the 19th century with the introduction of the thin blade saw (Hagman, O., 2013), in both Europe and North America. The technique is thought to have come to Sweden from

Norway (Thor, L. 2024). Similar techniques exist in other cultures, with examples of clay structures reinforced with perpendicular logs found in Korea and China (Roy, R., Flatau, R., 2015). The building technique today is mostly practiced by self-builders, but a couple of large-scale projects have used the technique for its favorable environmental properties and cost-effectiveness. Examples of this use is the Quetzal cordwood classroom in Coban, Guatemala by The Saskatoon architectural firm seen in *figure 1.2 a) (*Community Cloud Forest Conservation*,* no date*)* and the Arcus center for social justice leadership in the Kalamazoo, USA by Studio Gang Architects in 2014 seen in *figure 1.1 c) (ArchDaily, 2014)*.

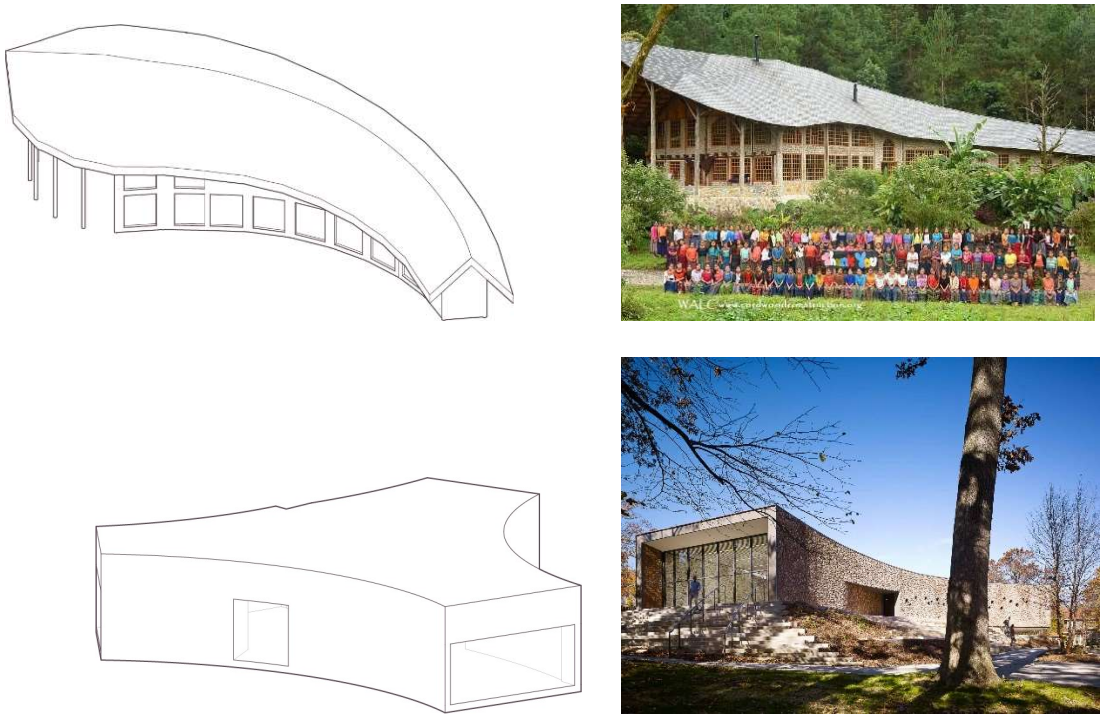

Figure 1.2: *Examples of contemporary large-scale cordwood projects a & b) Quetzal cordwood classroom c & d) Arcus center for social justice leadership*

Because of the ability to use material regardless of diameter and the short lengths necessary (often 30 to 40 cm), timber elements that are otherwise difficult to reuse or local trees can often be used.

Binders used today vary by region but the three most common are clay or cob, lime mortars and cement (Roy, R. 2016). Each has its own advantages and disadvantages. The most important properties of a binder are sufficient compressive- and bond strengths but other properties are used to differentiate which binder is most useful for the situation.

Clay binders have the lowest carbon footprint of these alternatives but have worse insulating properties since they need a continuous bond. Cement and lime mortar, allow for three partitioned bonds with one layer of an insulating material such as sawdust or foam. This is referred to as shell-bedded masonry. This gives these alternatives better thermal properties.

1.2.2 Prior work on cordwood

There are two main studies on the strength of cordwood; Mouterde, R., et al (2010) and Brics, A., et al (2022). Most other writings about the building technique focus on the historical use or acting as guides for self-builders.

The mechanical performance of cordwood by Mouterde, R., et al (2010) focused on testing the compressive strength of typical cordwood binders. This was done through laboratory testing of cordwood composite specimen. The sizes of the tested specimen were 0.6 x 0.4 x 0.3 m and 0.5 x 0.3 x 0.5 m.

Three types of binders were tested: clay-based earth mortar, non-hydraulic lime mortars and hydraulic lime mortars. For the lime binders in addition to testing the mortar with traditional aggregates such as sand, organic aggregates of sawdust, woodchips and hemp were tried. The proposed advantages of the organic aggregates were manifold, better thermal performance, lower embodied carbon dioxide, and better deformability. The mortars with organic aggregates were considerably weaker than the traditional lime mortars.

In addition to the compressive tests the paper discussed the topics of sustainability and thermal performance. Cordwood has low embodied carbon since very little machining or chemical processes are necessary to prepare the wood and it can utilize almost any log. This means that wood that otherwise would be burned because of its diameter or shape can still be utilized in construction, storing carbon dioxide instead of releasing it into the atmosphere.

The paper propositions that a binder with a larger proportion of organic aggregates could provide better thermal properties and lower embodied carbon dioxide. The material also was deemed to be strong enough for individual houses with a failure point of 1.5 MPa, which according to the paper is 10 times the downward force of a typical small house. This value was compared with un-stabilized rammed earth, an established alternative building material, that only reaches 0.8 - 1.5 MPa. The properties of the mortar were also deemed essential through observations of the drying process and the testing.

Brics, A., et al (2022) *The behaviour of Load-Carrying Members from Cordwood,* similar to the earlier work, investigated different binders through physical testing of cordwood composites and finite element modelling. The study proposes a formula for the strength of the cordwood entirely based on the strength of the mortar arguing that it is the loadbearing material. For mortars with a much higher stiffness and strength than wood this is plausible but for weaker mortars e.g. clay or the lignin mortars investigated in this study, this seems inadequate as the stress distribution will follow the stiffer material.

In the study binders were tested for compressive strength in isolation, as well as a part of cordwood composites. The physical testing of binders was carried out on 100 x 100 x 100 mm cubes. Lime binders, cement binders and clay binders were tested and measured compressive strengths of 36.76 MPa, 7.12 MPa and 1.94 MPa respectively.

The physical testing of cordwood was done on twelve 400 x 400 x 400 mm samples. The samples differed in terms of binder, shape of the wooden masonry units and if shell

bedded masonry was used. The mean compressive strength of the cordwood samples, in the same order as for the mortar tests, were 2.48 MPa, 1.51 MPa and 0.43 MPa. Their conclusion from this test was that the influence of mortar strength was limited. An increase in strength of the mortar does not correspond to an equivalent increase in cordwood strength and therefore the authors' reason that weaker mortars can be effectively used. This is consistent with the wooden masonry units influencing the strength of the masonry composite.

The study also established a finite element model of one of cordwood samples using a cement binder in ANSYS. The model is a so-called micro-model where the binder and masonry units are modelled separately. The results from the FE analysis followed the experimental results, e.g. showing high stress where cracks happened.

In addition to studying compressive strength the paper looked at fire action on cordwood structures. This was done purely through analytical means since no actual tests were performed.

Two North American authors that have written literature for self-builders. These are Rob Roy and Richard Flatau and they have each written one book claiming to be the definite guides to the subject in addition to other writings on specific projects. *Cordwood building: a comprehensive guide to the state of the art* (2016) by Rob Roy and *Cordwood Construction Best Practices* (2020) by Richard Flatau respectively.

Roy and Flateau have jointly hosted the Continental Cordwood Conference where contemporary cordwood projects are discussed. The two projects in chapter 1.2 are two examples from the 2015 edition of this conference and are published in Roy, R. & Flateau, R. (2015) *Continental Cordwood Conference Papers 2015.*

A contributor to the conference and author of the introductory chapter in Roy, R. (2016) is Olle Hagman. Hagman is a Swedish engineer, cordwood builder and hobby historian that has written two books about the subject in Swedish, *Väggar av ved: en bok om kubbhusen historia och möjligheter* (2013) and *Mura med ved* (2017). In these books he describes both the history of cordwood construction and some of his own experiments with the material as well as providing guidance for Swedish self-builders.

Szewczyk. J has written about historical cordwood construction in Europe with focus on Eastern Europe. His two primary works on the subject *Cordwood heritage* (2007) and *Building with Stovewood in Eastern Europe (c.1895 - 1965)* (2023) provides a historical context for the building technique but does not give much useful contemporary input for this thesis.

1.2.3 Properties of traditional binders

Three traditional binders in cordwood construction are clay, lime mortar, and cement mortar.

Clay mortars, also sometimes referred to as cob mortars or earth mortars, were used primarily in older constructions but are used even today in the natural building community as a more sustainable binder. Cement mortars are more common in contemporary constructions, lending a higher stiffness to the building. Cement binders are often so much stronger than the timber that the wall can be likened to a concrete

wall with the binder acting as the load bearing element rather than the masonry elements (Roy, R. 2016).

For all the binders the exact properties vary depending on the precise mixture. To be able to compare the lignin-sawdust binders with the traditional binders some general values are presented in table 1.1. The values for lime-sand and lime cement sand are taken from Soleymani, A., et al. 2022 and the values for clay/mud are taken from Becker, A., et al. 2024. These sources were chosen in addition to the more closely related study Brics, A., et al (2022), since the latter did not present any modulus of elasticity for the binders tested.

Table 1.1: *Properties of traditional binders*

Binder Type	E-modulus (MPa)	Compressive strength (MPa)	Poisson's Ratio	Density (kg/m3)
Lime-Cement-Sand*	6465	3.02	0.222	2069
Cement**	23000	25	0.2	2030
Clay***	3950	1.54	0.11	1924

Data from *Soleymani, A., et al. 2022 **Marques, A. I., et al. 2020 ***Becker, C., et al. 2024

Table 1.2: *Results from Brics, A., et al (2022)*

Binder Type	Compressive strength (MPa)
Lime	7.12
Cement	36.76
Clay	1.94

1.2.4 Previous work on lignin binders

An alternative binder was introduced by Olle Hagman (personal communication, 2025), made from sawdust, paper sludge and glue, and was further developed by this thesis authour in the thesis *Globwood: Cellulose-Glue Binder for Cordwood Masonry* (Stålhammar, O., 2025), expanding the recipe to include lignin. The new recipe, in the ratio 1:1:1:2 of volumetric parts, is paper sludge, starch-based glue, sawdust and lignin (shorthanded *SLL* in this report).

Hagman proposes another use for a lightweight binder being that it can allow prefabricated cordwood elements. He has experimented with traditional binders but found that the heavy binders made the pieces unwieldy.

In the author's thesis (Stålhammar, O., 2025), qualitative tests established that the new binder has better properties for environmental stability, assumed compressive strength and smoother surface finish than the one proposed by Hagman, while keeping the binder light and environmentally less damaging than lime mortars and cement. The binder is slightly heavier than the one only using sawdust and requires lignin which is not yet as readily available for private consumers.

A short two-week trial of environmental stability within Stålhammar, O. (2025), found that a binder with a mix of lignin and sawdust can last in an outdoor environment longer than the pure sawdust-based binder, but it was concluded that a longer study was necessary to establish if the binder can survive longer exposure.

1.2.5 Lignin as a resource

Lignin (or lignins) is a group of biopolymers present in plants, especially trees. It is the second most abundant macro molecule after cellulose. Lignin is a byproduct of existing industrial processes such as papermaking or biorefineries. Today nearly all lignin is burnt as low-value fuel. This makes it an interesting and exciting material for research and industry with over 5000 references between 2000 and 2018 in SciFinder Scholar. (Tribot, A., et al., 2019). Some examples of lignin uses being researched are:

Phenol formaldehyde is the most common adhesive for engineered wood products such as oriented-strand boards (OSB), plywood and laminated veneer lumber (LVL). Kalami, S., et al. (2017) successfully replaced phenol formaldehyde with lignin, creating a resin based on agricultural waste rather than petroleum products with no statistical loss in strength.

Boquera, L., et al. (2021) tested composite plaster boards where lignin replaced 30 – 100 % of gypsum. The article compared different composites thermal, mechanical and acoustic properties. Plaster boards with higher lignin content have better insulating properties but suffer in terms of mechanical strength and acoustic absorption for higher frequencies. The authors see potential in adding lignin to the plaster boards in limited quantities to create a material with a lower environmental impact.

Lignin has been investigated as a more environmentally friendly additive to stabilize silt to prepare the soil for construction. One paper that investigated this is Zhang, T., et al. 2016. The study found that 12 % lignin was the optimal level for stabilizing the soil in the geographic area for the study, changing the behavior from brittle to ductile.

1.3 Aim and research question(s)

Few studies have been conducted on modern applications of cordwood construction and even fewer have focused on developing new binders for wood masonry. This thesis therefore positions itself at the forefront of a new field.

The most important purpose of this thesis is to establish a basic understanding of the material to facilitate further interest in alternative binders for wood masonry.

The primary aim of this thesis is to establish some of the physical properties of the novel lignin binder through tests and finite-element models and to compare it with the known properties of the traditional binders (cement, lime mortar, clay binder).

Since very little is known about the material in structural applications, the main properties studied in this thesis are compressive strength, to determine if walls made with a reasonable thickness can withstand loading from a one-story building, and how the material is affected by environmental factors.

This narrows the thesis aim into the following four research questions

- What is the lignin binder's compressive strength and behavior when exposed to an outdoor environment?
- How does it compare with the traditional binders of cement, lime mortar and clay?
- Based on the above questions, where is it suitable to be used within a cordwood structure?
- Using the structure designed in Stålhammar, O. (2025) as an example, what dimensions are necessary (if possible) to achieve a structural sound building?

1.4 Limitations

As mentioned previously in the aim, this field of research is under explored which comes with both possibilities and limitations. Since very little is known about the material, the work done in this thesis covers a broad range of parameters rather than focusing on a single aspect. Since this thesis is not connected with the industry, practical concerns dominate the limitations. Due to limitations in amount of available raw material for the binder and the time allocated for this thesis means that the research presented
is intended as a starting point for further research rather than a conclusive endpoint.

The focus of the thesis is on testing the binder. No tests of cordwood composites were performed.

This thesis studies only four binder candidates, all with similar composition with the primary focus of the thesis being the two binders containing both lignin and sawdust.

The finite-element model (FEM) is limited in scope to the elastic interval and plastic redistribution of stresses and inner forces is not part of this thesis. The FEM also only considers pure vertical loading using a compressive force. No values for the interface behavior between the mortar and the log-ends are experimentally produced in this report. This means that the FEM is not used to determine the failure mode and is limited to looking at the distribution of stress and comparing it to the compressive strength.

Only calculations in ultimate limit state are performed.

2 Theory

This chapter aims to establish a foundation for the methods used in chapter 3.

Chapter 2.1. Strength of materials, the anisotropy of wood is discussed, and how materials can be tested. This includes both the methods chosen as well as some additional or alternative tests.

Chapter 2.2. Discusses some aspects of how materials can degrade.

Chapter 2.3. Is a short introduction to the finite element method with a focus on how it is used with regards to masonry constructions.

Chapter 2.4. Introduces what is said in Eurocode about masonry, the equations used to validate the FEM and the basis for the loads used.

2.1 Strength of materials

2.1.1 Timber and wood

Wood is an anisotropic material with different strength depending on the grain direction. Parallel, perpendicular, tangential. Normally only parallel and perpendicular are considered since tangential for most use cases is close to perpendicular. (Swedish Wood, 2020). Wood is much stronger parallel with the fibers than perpendicular to them. A true failure in compression perpendicular to the grain is impossible to define, with the ability for stress to further increase even after crushing has begun. The compressive strength for this case is defined as the stress level where 10 percent of deformation is still possible. This is usually between 3-5 MPa.

For cordwood construction loads act primarily in perpendicular and tangential directions.

2.1.2 Masonry binders and mortars

A masonry binder is typically made with an active binding agent, fibers and ballast where all parts contribute to the overall properties of the mortar. The binding agent can function through different means; through chemical reactions such as in the case of cement and lime, or through electrostatic properties and Van der Walls forces in the case of clay. The glue used in this project binds through a mix of chemical reactions and physical penetration of the wood.

The mix of particle sizes in the ballast contributes to the workability of the binder and the compressive strength. In the binders used in this project both sawdust and lignin act as ballast, with the fine lignin dust contributing with the small particle sizes and saw dust providing the larger particles.

Fibers contribute to the tensile strength of a binder; in these binders this effect is performed by the papersludge and the sawdust.

A binder does not necessarily need contribute with compressive strength to a building element, but all commonly used masonry mortars do. It can be enough that it contributes with bond strength similar to regular wood glue.

2.1.3 Compressive strength

Compressive strength is the maximum compressive stress a material can resist before cracking or being crushed. Masonry is primarily loaded with compressive loads meaning that compressive strength is usually the most important property of a masonry material. A higher compressive strength means that a building can be built taller. Since masonry materials usually are chosen with high compressive strength, compressive failure usually indicates poor material choice or a design flaw.

Compressive strength is tested through loading a specimen with a hydraulic ram until the material cracks. See figure 2.1 a).

2.1.4 Tensile strength

Tensile strength is very similar to compressive strength. It is the maximum tensile stress a material can take before it cracks or snaps. Tensile stresses are usually introduced in masonry from lateral forces such as wind loads acting on the wall. In cordwood masonry tensile stress can appear when the force path through the composite arches. A tensile failure could mean that cracks in the wall are created leading to increasing infiltration through the wall. Masonry is usually much weaker in tension than compression.

Tensile strength is tested through diagonal loading of a masonry composite or through the stretching of a material prism. See figure 2.1 b) and c).

2.1.5 Shear strength

Shear strength is a materials ability to resist internal sliding. A shear failure can happen in masonry constructions at the material level of either the mortar or the masonry unit, or as a bond failure at the interface.

Shear strength is tested through shearing a masonry prism or if the bond strength is higher than the shear strength, through the shearing of a masonry triple. See figure 2.1 d).

2.1.6 Bond strength

Bond strength is the adhesion between the binder and the masonry units. In the case of failure in the bond, the masonry composite stops acting as a continuous material. The failure can happen when the masonry composite is experiencing tensile or shear stress.

Bond strength can be measured through shearing of a masonry triplet or through a wrench test. See figure 2.1 d) and e).

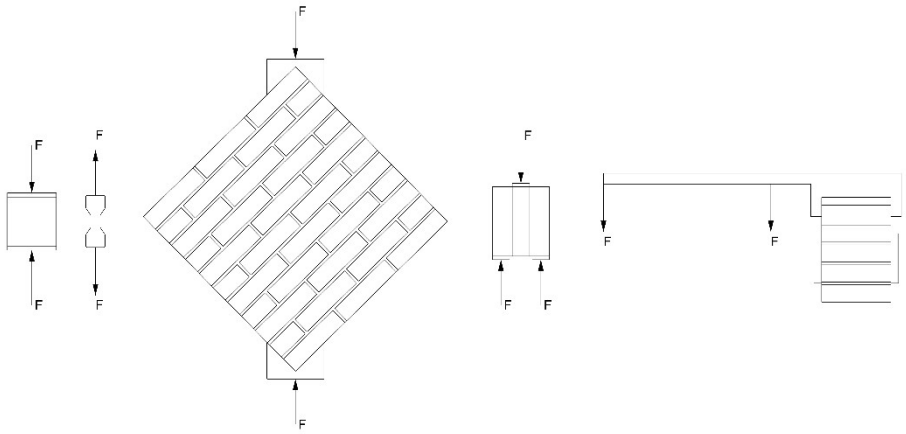

Figure 2.1: *From left to right a) compression loading b) tensile loading c) diagonal loading d) masonry triplet loaded in shear e) wrench test*

2.2 Degradation of building materials from environmental factors

All building materials risk degradation from exposure to the environment. Wind and physical wear from rain can damage the surface and remove material. Some materials such as unburned clay can dissolve in water. Trapped water in porous materials can freeze during cold periods causing frost wedging. This can be observed in concrete and masonry.

Cycles of wetting and drying for hygroscopic materials with moisture dependent volume risk introducing stresses. Similar effects can be observed from large changes in temperature. The risk further increases if two materials with very different behavior are bonded to each other.

For biological materials, additional risk comes from biodegradation. Rot and fungi attacks on wood-based building materials can critically impact the materials strength. Depending on the surface hardness of the material, animals and insects can damage it.

2.3 Finite element modelling

A Finite element model (FEM) is a numerical method for analyzing structures. The component to be analyzed (e.g. a building, a wall, or a car) is divided into a mesh containing information of the material's properties. Loads and boundary conditions are defined. The component's response is then simulated over a number of time steps until the model converges. A FEM is then able to show the stresses and displacements for every node in the mesh. A properly set-up FEM closely models the response of the analyzed component and can accurately predict cracks and stress distribution. Finite-element analysis (FEA) can be used for other types of simulations as well, including thermal transfer (convection, conduction), mass diffusion and acoustics. Some FEA software also allows simulation of fluid dynamics.

2.3.1 ABAQUS

ABAQUS is a commercial finite element software package under the SIMULIA brand. There are three main parts to ABAQUS: ABAQUS/standard, ABAQUS/explicit, and

ABAQUS/CAE. ABAQUS/standard is a general-purpose finite-element solver best at simulating static events or dynamic responses, compared with ABAQUS/explicit which is optimized as an explicit-dynamic finite-element solver best for much briefer events such as a crash or an impact. ABAQUS/CAE is an environment for modelling and visualizing FEA. The provided graphic-user-interface (GUI) makes it easier for newer users to navigate through the process while still being a useful tool to experienced users. Both ABAQUS/standard and ABAQUS/explicit are supported in ABAQUS/CAE.

2.3.2 Finite element modelling of masonry walls

There are two main techniques for numerical modelling of masonry walls. (Maria D'Altri, A., et al. 2018). Micro models and macro models. The difference between the modelling techniques makes them suitable for different applications and they also require different types of data to be known for their implementation. Maria D'Altri, A., et al. looked at how detailed micro models could be implemented from only knowing the material parameters of the constituent elements (bricks and mortar), and the interface between them from small scale tests.

Macro-modelling models the composite of the masonry units and the mortar using the combined properties of the two. For larger structures macro-modelling is the only computational practical method of modelling but requires the composite properties to be known.

Micro models can further be sub categorized into detailed micro models and simplified or discrete micro models. Maria D'Altri, A., et al. further distinguishes between detailed and continuous micro models.

Detailed micro-modelling models the masonry units and mortar separately. In addition, the interface between the materials can be specified separately. Micro-modelling is only computationally practical for small structures.

Simplified micro-modelling models the masonry units expanded to include the mortar joints. The interface between the masonry units is based on the properties of the mortar. Simplified micro-modelling is the preferred method for detailed modelling when the combined properties of the mortar and the masonry units are known.

In this thesis, where the focus is on the binder, detailed micro-modelling is the method that is chosen.

2.4 Requirements in Eurocode

The relevant parts of Eurocode for this thesis are SS-EN 1996 which deals with masonry structures discussed in **chapter 2.4.1**, and SS-EN 1991 about loads and actions on structures discussed in **chapter 2.4.2**.

2.4.1 Masonry structures

The design of masonry structures is discussed in SS-EN 1996-1-1:2022. Chapter 5.7 discusses the mechanical properties of masonry, and the following formulas are collected from there.
A masonry walls' compressive strength is dependent on the strength of the mortar and the masonry units. For non-shell bedded masonry.

$$f_k = K f_b^{\alpha} f_m^{\beta}$$ eq. 1

Where:

K is a parameter that is unknown for cordwood but the range for other combinations of binders and masonry units is 0.20 - 0.80

f_b is the compressive strength of the masonry units. [N/mm2]

f_m is the compressive strength of the mortar [N/mm2]

α is a constant related to f_b that depends on the bond type.

β is a constant related to f_m that depends on the bond type.

For a masonry wall using general purpose or lightweight mortars can be calculated

$$f_k = K f_b^{0.7} f_m^{0.3}$$ eq. 2

Chapter 8.2 discusses the verification of unreinforced masonry walls subjected to primarily vertical loading, in the ultimate limit state, which is the case that will be discussed in this thesis.

$$N_{Ed} \leq N_{Rd}$$ eq. 3

$$N_{Rd} = \phi t f_d$$ eq. 4

Where:

t is the thickness of the wall.

ϕ_i is the reduction factor for the top and bottom of the wall taking account for eccentricity and slenderness

$$f_d = f_k / \gamma_M$$ eq. 5

Where:

f_k is the compressive strength from eq. 1 or eq. 2 [N/mm2]

Reduction factor for any mortar with Category II units, $\gamma_M = 2.5$

$$\phi_i = 1 - \frac{2e_i}{t}$$ eq. 6

$$e_i = \frac{M_{id}}{N_{id}} + e_{he} + e_{init} \geq 0.05t$$ eq. 7

Where:

M_{id} is the design value of the moment at the top or bottom

N_{id} is the design value of the vertical load at the top or bottom

e_{he} is the eccentricity at the top or bottom of the wall, if any, resulting from horizontal loads

e_{init} is the initial eccentricity with a sign that increases the absolute value of e_i.

A simplified calculation can be performed according to SS-EN 1996-3:2024 for walls subjected to vertical and wind loading, where eq. 4 is modified as follows.

$$N_{Rd} = \phi_s t f_d l$$ eq. 8

Where ϕ_s for end supports is

$$\phi_s = min\begin{cases} 0.85\ \frac{t_b}{t} - 0.0011\left(\frac{h_{ef}}{t}\right)^2 \\ \left(1.2 - \frac{l_{f,ef}}{l_{ref,c}}\right)\frac{t_b}{t} \geq 0.33 \\ \left(1.2 - \frac{l_{f,ef}}{l_{ref,t}}\right)\left(\frac{t_b}{t}\right)^2 + 0.09\left(\frac{t_b}{t}\right)\left(\frac{h}{t}\right) \geq 0.33 \end{cases} \quad \text{eq. 9}$$

Where:

h_{ef} is the clear height of the wall.

t is the thickness of the wall.

t_b is the bearing length of the floor on the wall.

$l_{f,ef}$ is the difference of the effective span of the floors in meters on both sides of the considered wall.

$l_{ref.c}$ value depending on the characteristic compressive strength of the masonry f_k, the ratio E/f_k and the thickness of the wall t. See table 2.1.

$l_{ref,t}$ value depending on the characteristic compressive strength of masonry f_k and the thickness of the wall t. See table 2.1.

$$l_{f,ef} = l_{f,ef,1} - l_{f,ef,2} \geq 3.00\ m \quad \text{eq. 10}$$

$l_{f,ef,i,}$= 0.9 $l_{f,I}$ for simply supported floors

Table 2.1 *Reference values for $l_{ref.c}$ and $l_{ref,t}$. Values for $l_{ref.c}$ are valid for $E/f_k > 600$.*

f_k (N/mm2)	$l_{ref,c}$ (m)	$l_{ref,t}$ (m)	
		t ≤ 300 mm	t = 500 mm
$f_k = 1$	8,00	2,8	3,7
$f_k \geq 5$	9,50	4,4	8,1
Linear interpolation may be carried out between 1 N/mm^2 < f_k < 5 N/mm^2 as well as between 300 mm < t < 500 mm..			

For $E/f_k \leq 600$, $l_{ref.c} = 9.5\ m$.

2.4.2 Load cases in the structure

There are two main limit states in Eurocode that need to be considered for a structure to be deemed fit for purpose. Ultimate limit state (ULS) deals with safety and structural failure and service limit state (SLS) where unsatisfactory behavior is considered before failure. In this thesis only ultimate state is considered.

The basis of structural design is discussed in SS-EN 1990:2002. Chapter 6.4 in the code deals with the ultimate limit state with chapter 6.4.3 discussing load combinations.

The load combinations for one permanent load and one medium term load

$$LC = \gamma_d(1.2\ G_k + 1.5Q_{k,1})/k_{mod,med} \quad \text{eq. 11}$$

Where:

γ_d is the partial coefficient depending on the safety parameter, see table 2.2.

ψ_2 is the frequent value for variable loads, see table 2.3.

ψ_1 is the quasi-permanent value for variable loads, see table 2.3.
$k_{mod,i}$ is the partial coefficient for different climate classes, see table 2.4.

Table 2.2: *Safety parameters for load cases.*

Safety		γ_d
1 – Low	Low risk for severe damage to people	0.83
2 – Normal	Risk for severe damage to people	0.91
3 – High	High risk for severe damage to people	1

Table 2.3: *Combination values for variable loads depending on load duration.*

	ψ0	ψ1	ψ2
Snow Load			
$s_k \geq 3$ kN/m^2	0.8	0.6	0.2
$2.0 < s_k < 3.0$ kN/m^2	0.7	0.4	0.2
$1.0 < s_k < 2.0$ kN/m^2	0.6	0.3	0.1

Table 2.4: *kmod for different climate class*

Material	Climate Class	Load Duration				
		Permanent	Long	Medium	Short	Instant
Construction timber	1	0.6	0.7	0.8	0.9	1.1
	2	0.6	0.7	0.8	0.9	1.1
	3	0.6	0.55	0.65	0.7	0.9

In this thesis the k_{mod} for timber products is used since no value is known for the binder material.

2.4.2.1 Self-weight

Permanent loads such as densities, self-weight and imposed loads for buildings are discussed in SS-EN 1991-1-1:2002. In this thesis no imposed loads are present on the walls so only the densities of the building materials are considered as permanent loads. The walls are constructed with pine log-ends and one of the binder candidates that are discussed in this thesis. The densities of these materials are listed as follows.

Density of pine $\rho_{pine} = 450\ kg/m^3$
Density of binder $\rho_{SLL} = 400\ kg/m^3$
$\rho_{SSL} = 330\ kg/m^3$

2.4.2.2 Snow-load

The process for dimensioning for snow-load is described in SS-EN 1991-1-3.
The snow-load is defined as:

$$s = \mu_i C_e C_t s_k\ [kN/m^2] \qquad \text{eq. 12}$$

Where:
μ_i is the form factor.
Ce = 1.0 or 1.2 is the exposure factor for normal or sheltered areas respectively.
Ct = 1.0 is the thermal coefficient given by national standards.

sk = 1.5 kN/m2 is the characteristic snow-load in the Stockholm region.

The formfactor for vaulted roofs is defined in the standard in chapter 5.3.5. Depending on the roof angle β.

$$\text{For } \beta > 60°,\ \mu_3 = 0 \qquad \text{eq. 13a}$$

$$\text{For } \beta \leq 60°,\ \mu_3 = \min [0.2 + h/w,\ 2.0] \qquad \text{eq. 13b}$$

Where h is the height of the vault and w is the width of the vault. See figure 2.2.

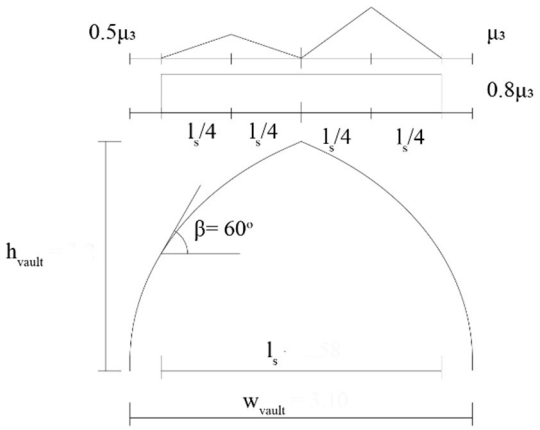

Figure 2.2: *Snow load*

3 Method for physical tests

The purpose of the physical testing is to determine the compressive strength of the binder to be used for comparison between the traditional materials and to be used as the basis for digital models and calculations. In addition, information on how the material fares when exposed to an outdoor environment or wetting is collected to be used in a discussion about the material's suitability.

3.1 Preparation of test specimens

The recipes for the mixtures use the volumetric proportions 1:1:3 of wallpaper paste, paper sludge and ballast. The ballast varies depending on the specific recipe. The paper sludge is a mix of newspaper and paper-towels cut into pieces, soaked in water and finally further slurried with a paint mixer. The types of ballast that are used are sawdust and lignin. The sawdust is of mixed particle sizes and materials recycled from a wood workshop vacuum system. The lignin is donated by Södra and come as a fine powder. No prior conditioning of the ingredients was done prior to the mixing, except soaking of the paper.

LLL: Binder recipe using three parts lignin as the ballast.
SLL: Binder recipe using one part sawdust and two parts lignin as the ballast.
SSL: Binder recipe using two parts sawdust, one part lignin as the ballast.
SSS: Binder recipe using three parts saw dust as the ballast.

Figure 3.1: *The materials used for the binder a) Wallpaper paste b) Lignin powder c) Sawdust*

The mix ratio of newspaper and paper-towels varied between batches, as did the time the paper sludge soaked in water.

The eight test cubes for the medium-term exposure test and the four test cubes for compression test: unmodified specimen are cast in wooden formwork with an inner dimension of 100 x 100 x 100 mm, see *figure 3.2*. The formwork was removed after one week of drying to allow the material to stabilize. All samples dried for a minimum of two additional weeks before the testing was performed. The drying conditions were room temperature, indoor environment.

The test cubes for the exposure test were casted in the early spring of 2025 for use in Stålhammar, O., 2025 and were stored in a heated indoor environment until the start of the summer. This experiment uses cubes made according to the LLL, SLL, SSL, and SSS recipes using the same method as above.

Figure 3.2: *a) Diagram over cube formwork b) Casted samples*

The material is expected to be isotropic due to the fiber direction being randomized in the mixing process. Some small amounts of anisotropic behavior could have been introduced in the casting process. Care was taken to try to fill the formwork without layering the material but due to the nature of the formwork one side was more exposed to air in the beginning in the drying process. This is noted but not expected to make much difference. For the cubes the direction perpendicular to the exposed side is used as length. For rectangular specimen the largest dimension is taken as length.
Since the behavior is expected to be anisotropic, other directional measurements (width, thickness) of the material are used arbitrarily.

3.2 Compression test: Unmodified specimen

The purpose of this experiment was to determine the compressive strength and the modulus of elasticity of the material.

The test cubes for compression test: unmodified specimen were made according to the SLL and SSL recipes; the samples were prepared 6 weeks before testing.

Compressive strength was tested through loading in a Universal testing machine, Tram UCT 50 kN, that can measure displacement and applied force see *figure 3.3*. The samples were tested until failure, and a stress-strain curve was calculated and plotted from the collected data in addition to noting the maximum compressive stress.

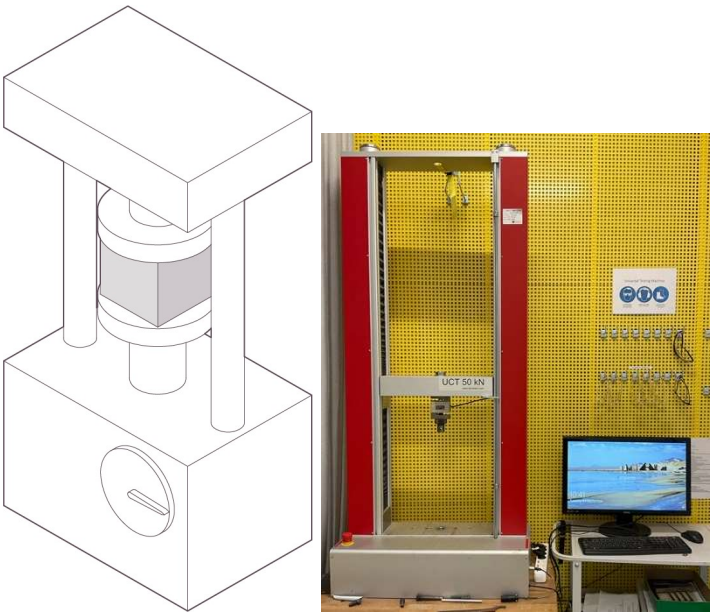

Figure 3.3: *a) Sketch of test setup for compressive load test. b) Photo of test setup*

The machine uses two square steel compression plates with a side length of 120 mm. See figure 3.4.

The speed during the test was 3 mm/min, but a faster speed of 10 mm/min was used until the compression plates reached a contact load of 2 N. After concluding the test, the plates had a retraction speed of 300 mm/min.

The maximum distance the plates was set to travel was 20 % of the length of test cube and the minimum distance was set to 1 mm. The maximum load the machine can provide is 50 000 N. The machine automatically stops the test when the applied force drops.

Figure 3.4: Test setup during testing procedure

The tests were documented with a timelapse in addition to the force and displacement data logged by the machine. The machine measures applied force using a load cell and can apply force with a resolution of 0.25 N according to the manufacturer. The

displacement is measured through the movement of the travelling beam and has a specified resolution of 0.0001 mm.

From the results of the compression test effective strength of the masonry composite is calculated using equation 1 (chapter 2.2). This value is compared with the loads from the structure (calculated in chapter 3.4.1).

The compression test was performed on 100 x 100 x 100 mm cubes. Two specimens of SLL and two specimens of SSL were used with dimensions according to table 3.1.

Table 3.2: *Compression Test: Unmodified specimen Dimensions*

	Dimensions				
	Dimensions			Mass	ρ
	mm	mm	mm	g	kg/m3
SLL 1	96,8	96,9	97,1	407	447
SLL 2	95,6	97,1	98,9	424	462
SSL 1	94	94,3	92,8	318	387
SSL 2	93,3	93,8	96,6	332	393

3.3 Exposure tests

Two different exposure tests were used to simulate different situations and durations. One multi-month outdoor test was complimented with a shorter but more intense test.

3.3.1 Medium-term exposure test

The purpose of the test was to see how the material stands up to being in an outdoor environment, to determine if the material is suitable for outdoor use. The experiment also aimed to see if a roof impacts the behavior of the material.

Environmental stability was tested by exposing the test cubes to an outdoor environment. Two cubes of each material mixture were placed in similar outdoor conditions, with one sample protected from direct rain with a roof structure while the other sample is exposed to the weather, See figure 3.5 and 3.6. The test cubes were photographed, and a tactile-visual inspection was performed at regular intervals.

The test duration was 2.5 months, from the middle of June to the end of August during the summer of 2025. The tests were performed in the northeast of Uppland, Sweden.

The weather data for the period was retrieved from SMHI using the closest active weather station (Örskär A, SMHI.se).

Figure 3.5: *Unsheltered specimen. From left to right LLL, SLL, SSL and SSS.*

Figure 3.6: *Semi-sheltered specimen. From left to right LLL, SLL, SSL and SSS.*

3.3.2 Aggravated wet-dry experiment

In addition to the in-situ exposure test, a shorter term but more extreme exposure test "aggravated wet-dry experiment" was performed. The experiment aimed to understand how wetting and drying of the material mixtures affected the material properties and behavior, depending on the duration of the wetting and drying, and establish if this behavior can differentiate between the material mixtures.

The test specimens for the aggravated wet-dry experiment were cut from 100 x 100 x 20 mm blocks created for Stålhammar, O., 2025 in the spring of 2025. The procedure is otherwise the same as for the 100 x 100 x 100 mm test cubes. Similar to the specimen in the exposure test, the material is stored in a heated indoor environment until the test is performed.

The specimens were submerged in water for between 1 and 72 hours and observed for 72 hours of drying after the soaking.

The use case for the material is primarily walls which means that the material is not expected to be submerged for long durations. This means that the short or medium durations show more realistic scenarios.

Procedure:

1. For every specimen the weight and dimensions are measured and recorded
2. All specimens, except one of each mixture (the control) are placed in containers filled with a layer of water.
3. After one hour, the first specimen of each mixture is removed from the container and placed to dry. The immediate dimensions are measured and compared with the control, in addition visual and tactile changes are also noted. The properties and dimensions are measured and compared with the control and are noted again after one hour, eight hours, twenty-four hours and seventy-two hours.
4. Step two is repeated for a new specimen after four hours of wetting, eight hours of wetting, twelve hours of wetting, twenty-four hours of wetting, forty-eight hours of wetting and seventy-two hours of wetting. See table 3.2: Experiment timeline

Table 3.2: *Experiment timeline*

Time (hours from start of the experiment)	**Control**	**Spec 1**	**Spec 2**	**Spec 3**	**Spec 4**	**Spec 5**	**Spec 6**	**Spec 7**
0	Drying	Wet	Wet	Wet	Wet	Wet	Wet	Wet
1		Drying						
2		Test 1 h						
4			Drying					
5			Test 1 h					
8				Drying				
9		Test 8 h		Test 1 h				
12			Test 8 h		Drying			
13					Test 1 h			
16				Test 8 h				
20					Test 8 h			
24						Drying		
25		Test 24 h				Test 1 h		
28			Test 24 h					
32				Test 24 h		Test 8 h		
36					Test 24 h			
48						Test 24 h	Drying	
49							Test 1 h	
56							Test 8 h	
72							Test 24 h	Drying
73		Test 72 h						Test 1 h
76			Test 72 h					
80				Test 72 h				Test 8 h
84					Test 72 h			
96						Test 72		Test 24 h
120							Test 72	
148								Test 72 h

3.3.3 Compression test: Impact of wetting

The compression test was performed on the specimen used in the aggravated wet-dry experiment. The purpose of the test was to determine how the wetting experiment impacted on the strength of the material.

The same machine settings were used for this compressive test as for the compressive strength test in chapter 3.1.2. The dimensions of the specimen are presented in table 3.3.

Table 3.3: *Specimen for compression test: impact of wetting*

Specimen		Dimensions [mm]	Weight [g]	Density [kg/m3)
SSS	Spec SSS0	45.0 x 20.2 x 21.3	5	259
	Spec SSS1	48.3 x 20.0 x 20.7	5	250
	Spec SSS2	42.6 x 20.4 x 20.7	5	279
	Spec SSS3	51.6 x 20.6 x 21.9	6	258
	Spec SSS4	41.8 x 20.5 x 21.2	5	275
	Spec SSS5	45.5 x 19.7 x 18.5	5	302
	Spec SSS6	50.7 x 18.8 x 20.0	5	262
	Spec SSS7	46.7 x 21.0 x 20.3	5	251
SSL	Spec SSL0	49.9 x 18.3 x 20.2	6	325
	Spec SSL1	48.5 x 20.4 x 20.0	7	354
	Spec SSL2	44.7 x 20.7 x 19.1	6	339
	Spec SSL3	49.1 x 19.8 x 20.7	6	305
	Spec SSL4	48.4 x 20.8 x 19.8	7	352
	Spec SSL5	44.6 x 20.9 x 19.6	6	328
	Spec SSL6	44.4 x 20.5 x 18.6	6	354
	Spec SSL7	43.8 x 20.4 x 19.3	7	406
SLL	Spec SLL0	46.2 x 19.9 x 17.9	7	425
	Spec SLL1	47.5 x 20.4 x 19.7	8	419
	Spec SLL2	46.0 x 20.4 x 17.9	7	417
	Spec SLL3	47.5 x 20.5 x 17.9	7	402
	Spec SLL4	47.0 x 20.1 x 18.2	7	407
	Spec SLL5	46.2 x 20.5 x 18.2	7	406
	Spec SLL6	47.3 x 20.8 x 18.8	6	324
	Spec SLL7	48.0 x 20.7 x 19.1	8	422
LLL	Spec LLL0	46.1 x 20.9 x 20.0	8	415
	Spec LLL1	46.0 x 20.5 x 19.3	8	439
	Spec LLL2	49.6 x 20.4 x 20.2	9	440
	Spec LLL3	44.4 x 20.8 x 19.6	7	387
	Spec LLL4	45.9 x 21.3 x 19.5	8	420
	Spec LLL5	47.6 x 20.5 x 19.0	9	485
	Spec LLL6	46.5 x 20.5 x 19.6	8	428
	Spec LLL7	45.5 x 19.9 x 19.2	7	403

4 Results

Chapter 4 shows the results of the physical experiments.
Chapter 4.1 focuses on the compressive test of the unmodified specimen while **chapter 4.2** focuses on the exposure tests.

4.1 Compressive strength

Compression test: Unmodified specimen
The results from compression test: unmodified specimen is presented in tables 4.1 and 4.2 and figures 4.2 and 4.3. The results indicate a material with low stiffness and low maximum strength. Figure 4.1 shows a photo from the test showing how a compressive failure can look.

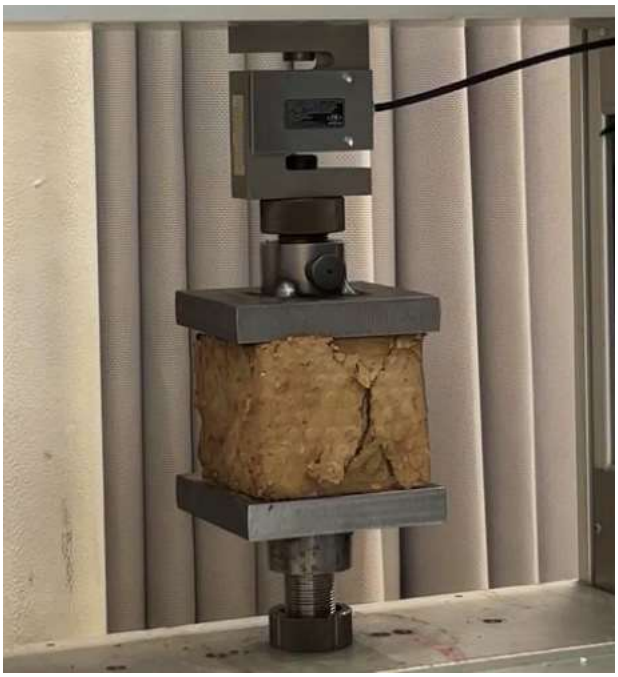

Figure 4.1: *Compression failure of SLL test cube*

Table 4.1 shows the maximum force applied to the specimen and the corresponding stress in the specimen. The displacement is taken from the moment of maximum stress. The E-modulus is calculated using the tangent in the elastic area. Table 4.2 shows the same results averaged by material. The maximum stress is similar between the materials, 0.393±0.013 for SLL and 0.402±0.025 for SSL. The spread of displacement at the maximum stress shows large variation even within material mixtures, the 2nd SLL specimen more than doubled the displacement from the 1st SLL specimen.

Table 4.1: *Compression test: Unmodified specimen Results*

	Results			
	Max Force	Max σ	ϵ(Max σ)	E-modulus
	N	N/mm^2	-	N/mm^2
SLL 1	3572	0.381	0,045	12.82
SLL 2	3764	0.406	0,095	14.53
SSL 1	3344	0.377	0,07439	9.25
SSL 2	3737	0.427	0,100	6.61

Table 4.2: *Compression Test: Unmodified specimen Average Results*

	Average			
	Max F	Max σ	ϵ(Max σ)	E-modulus
	N	N/mm^2	-	N/mm^2
SLL	3668	0.393	0.070	13.68
SSL	3540	0.402	0.087	7.93

Figures 4.2 and 4.3 show the results as graphs, plotting the force and stress respectively over displacement. The graphs are all similar, but a noticeable difference can be seen between material mixtures showing that the different mixtures do influence the binders' properties. The SLL specimens show a steeper gradient of the stress-strain curve than the SSL specimens indicating a higher modulus of elasticity.

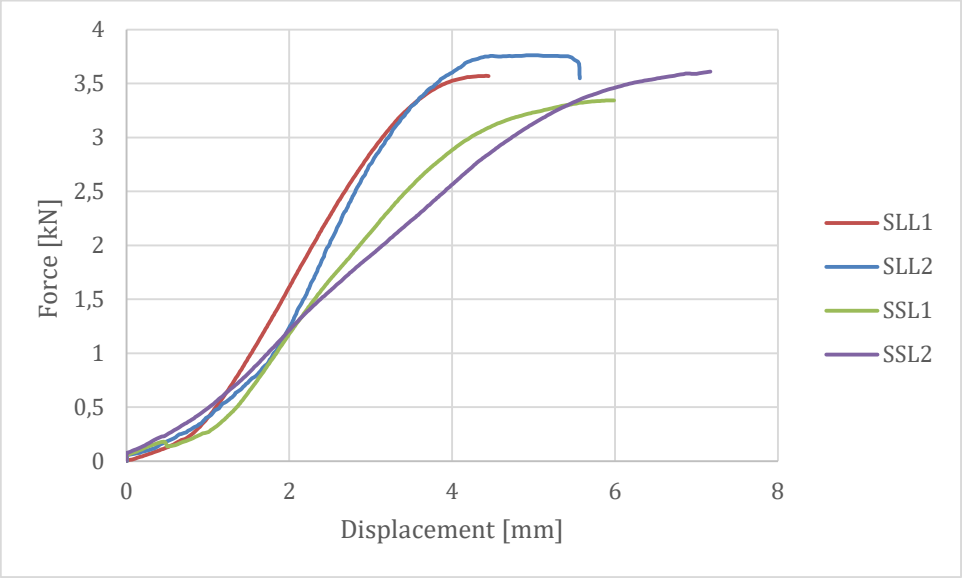

Figure 4.2: *Force/Displacement Compression test: Unmodified specimen*

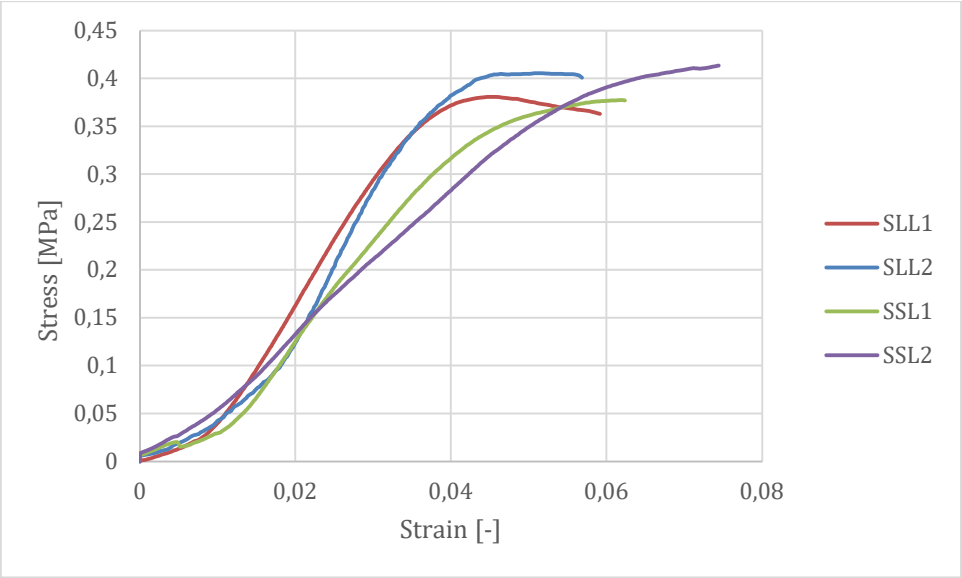

Figure 4.3: *Stress/Strain Compression test: Unmodified specimen*

4.2 Exposure tests

4.2.1 Medium term exposure test

Fifty observations over the course of eighty days (2025-06-14 to 2025-09-01) showed how the cubes reacted to the environment. The cubes in the semi-exposed environment showed signs of surface level cracks in the *LLL* and the *SLL* samples but there was no noticeable reduction in stability. The cubes in the fully exposed environment showed much more noticeable changes with the *LLL* and *SSS* samples mostly disintegrating after forty days. The *SLL* sample showed slight damage but remained as a mostly intact cube for the entire duration of the experiment. The *SSL* sample was seriously damaged but remained partially intact. Figure 4.4 shows the specimen at the start and end of the experiment, with a larger number of images being shown in appendix I: Photos from medium-term exposure test.

The weather during the experiment is shown in figures 4.5 and 4.6. The lowest temperature measured was 9.6 °C while the average temperature during the period was 16 °C. In total it rained for 26 days during the experiment

Figure 4.4: *a) Partially sheltered samples at the start of the experiment b) Exposed samples at the start of the experiment c) Partially sheltered samples at the end of the experiment d) Exposed samples at the end of the experiment*

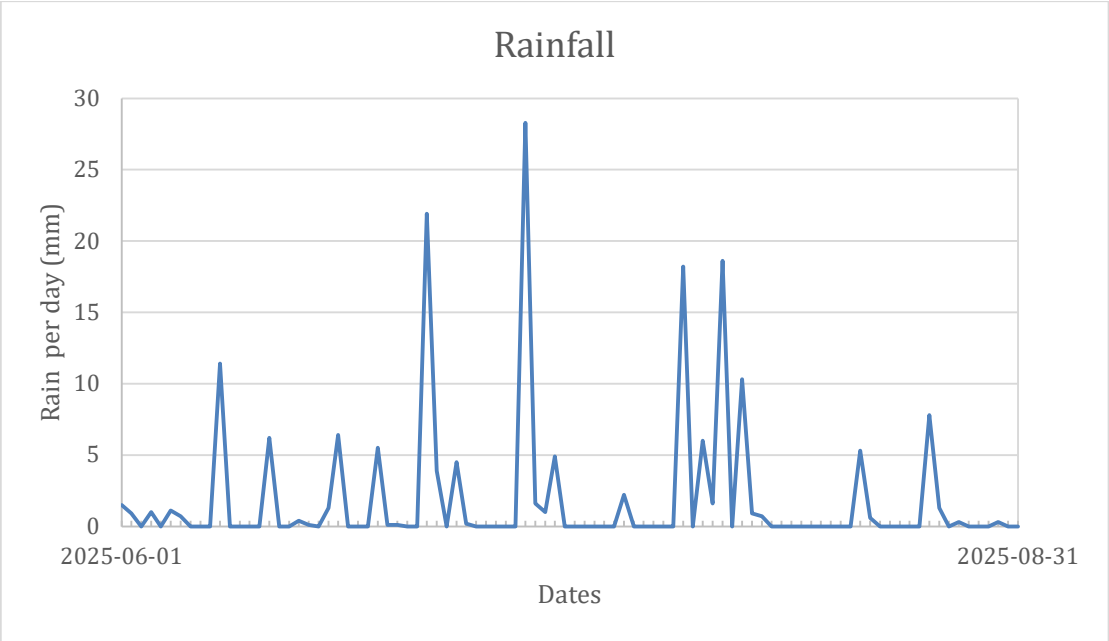

Figure 4.5: *Daily rainfall during the experiment period.*

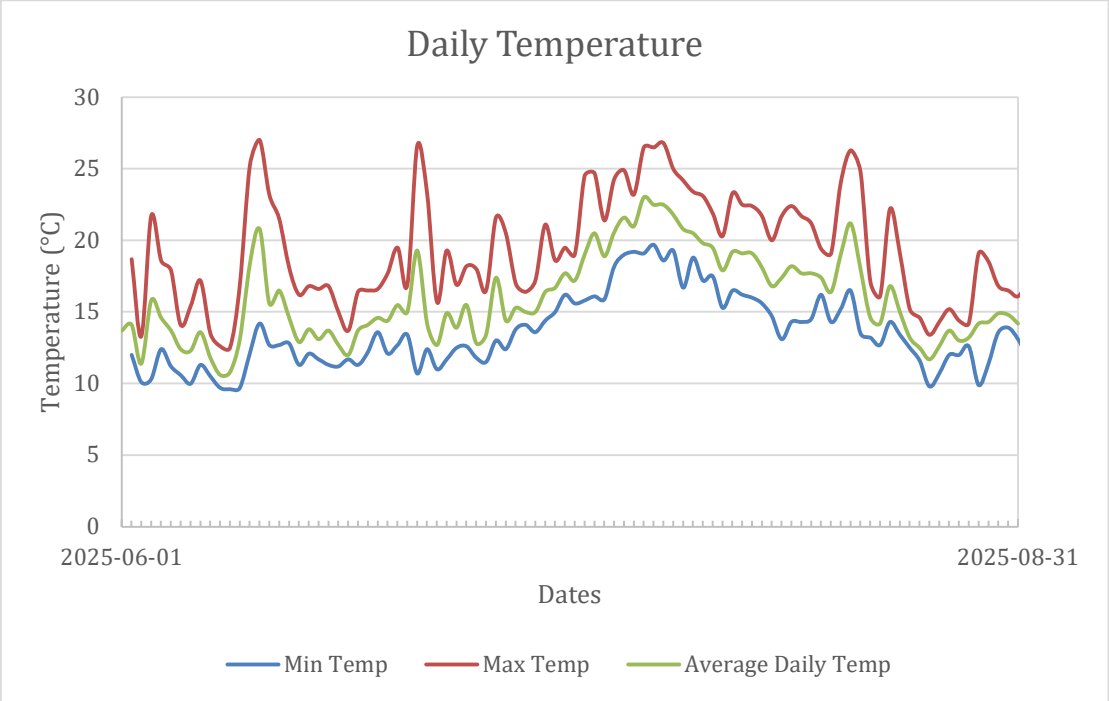

Figure 4.6: *Minimum, maximum and average daily temperature in the area during the experiment period.*

4.2.2 Aggravated wet-dry experiment

The result of the experiment is highlighted in figures 4.7 through 4.12.

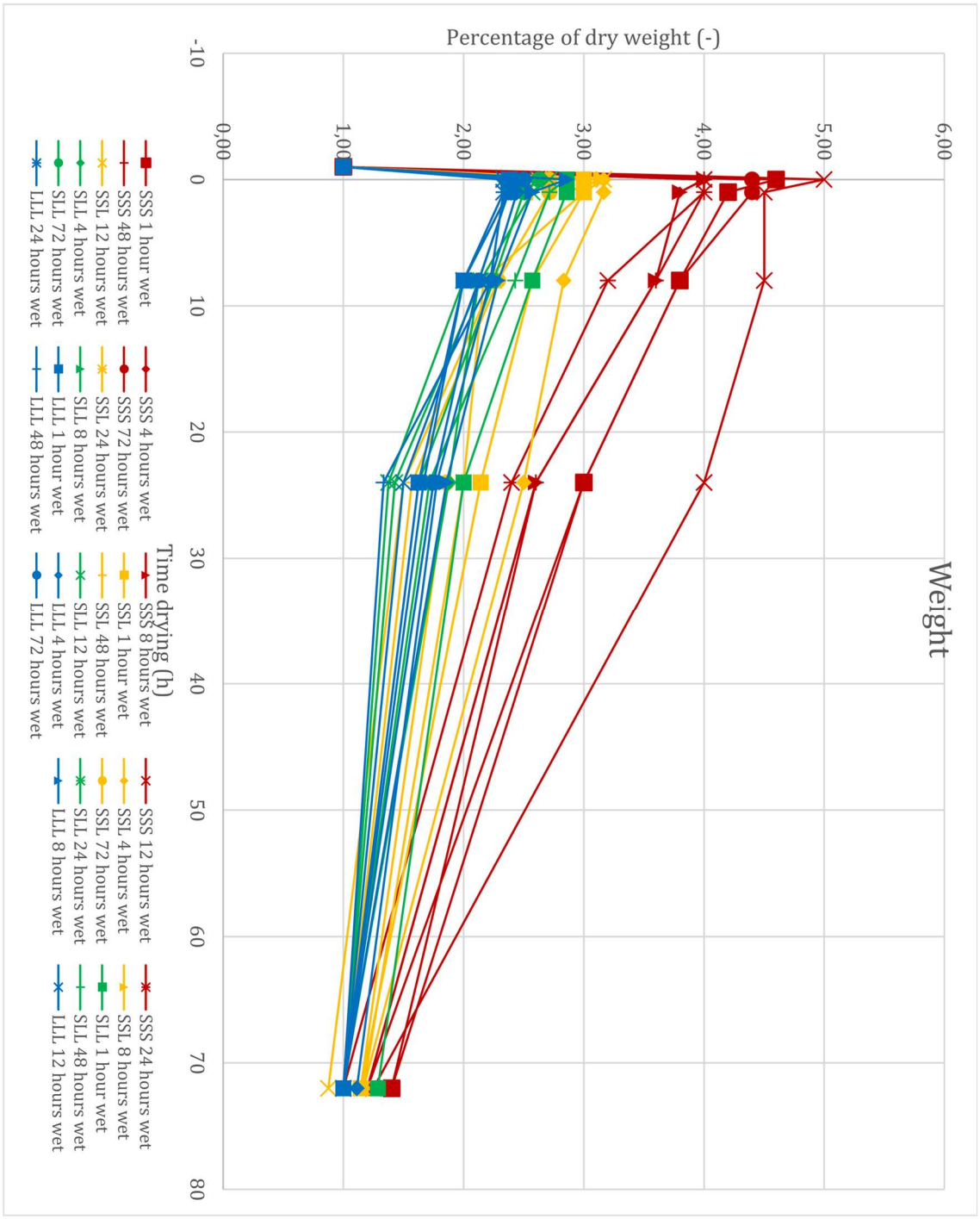

Figure 4.7: *Normalized weight over time while drying for different lengths of wetting. The color of the marker indicates how long the specimen was in the water while the shape of the marker indicates the material composition.*

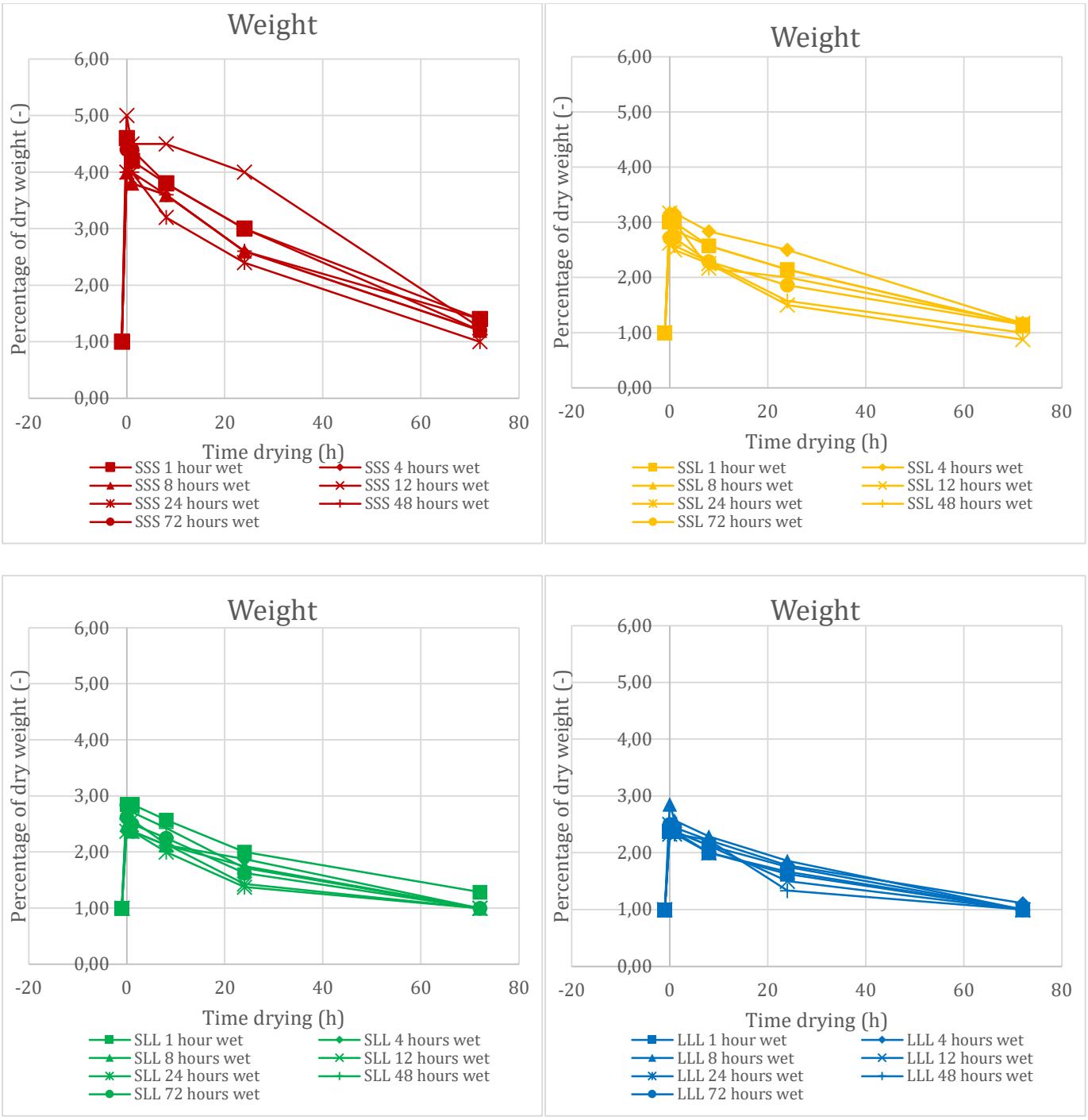

Fig 4.8: *Weight over time separated by material mixture a) SSS b) SSL c) SLL d) LLL*

Figure 4.7 and 4.8 shows the weight of the specimen compared with the dry weight of the specimen. The result indicates that SSS absorbs more water than other material mixtures. All mixtures are close to fully dry after 72 hours of drying regardless of how long they have been in water meaning that the specimens are saturated after 1 hour of wetting. This is even easier to see in figure 4.9 showing an almost horizontal trendline for all mixtures in the amount of water the specimen has absorbed for different amounts of time wet.

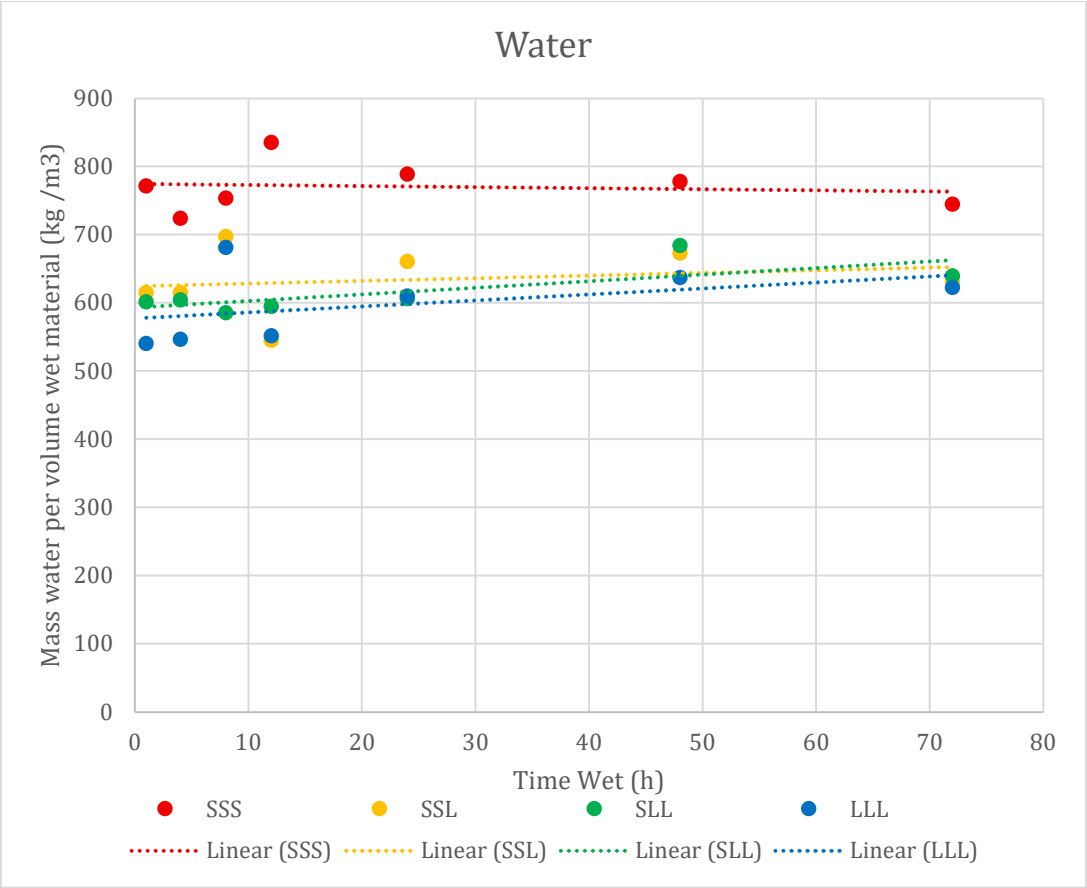

Figure 4.9: *The difference between the weight immediately after removing from the water and the dry weight divided by the volume of the wet material*

Figures 4.10 and 4.11 show the change in volume during the drying process. Most specimens return to 100 % of the starting volume but a few specimens show a smaller volume in the end.

A smaller volume in the end can indicate that the specimen has lost material during the wetting process, due to dissolving in the water. This is consistent with the result that the specimen who were in the water for the longest (72 h) indicated with light blue in the figure shows the largest loss in volume. Up to 20 % lower volume was measured in the end which would result in a lower area and increased stress.

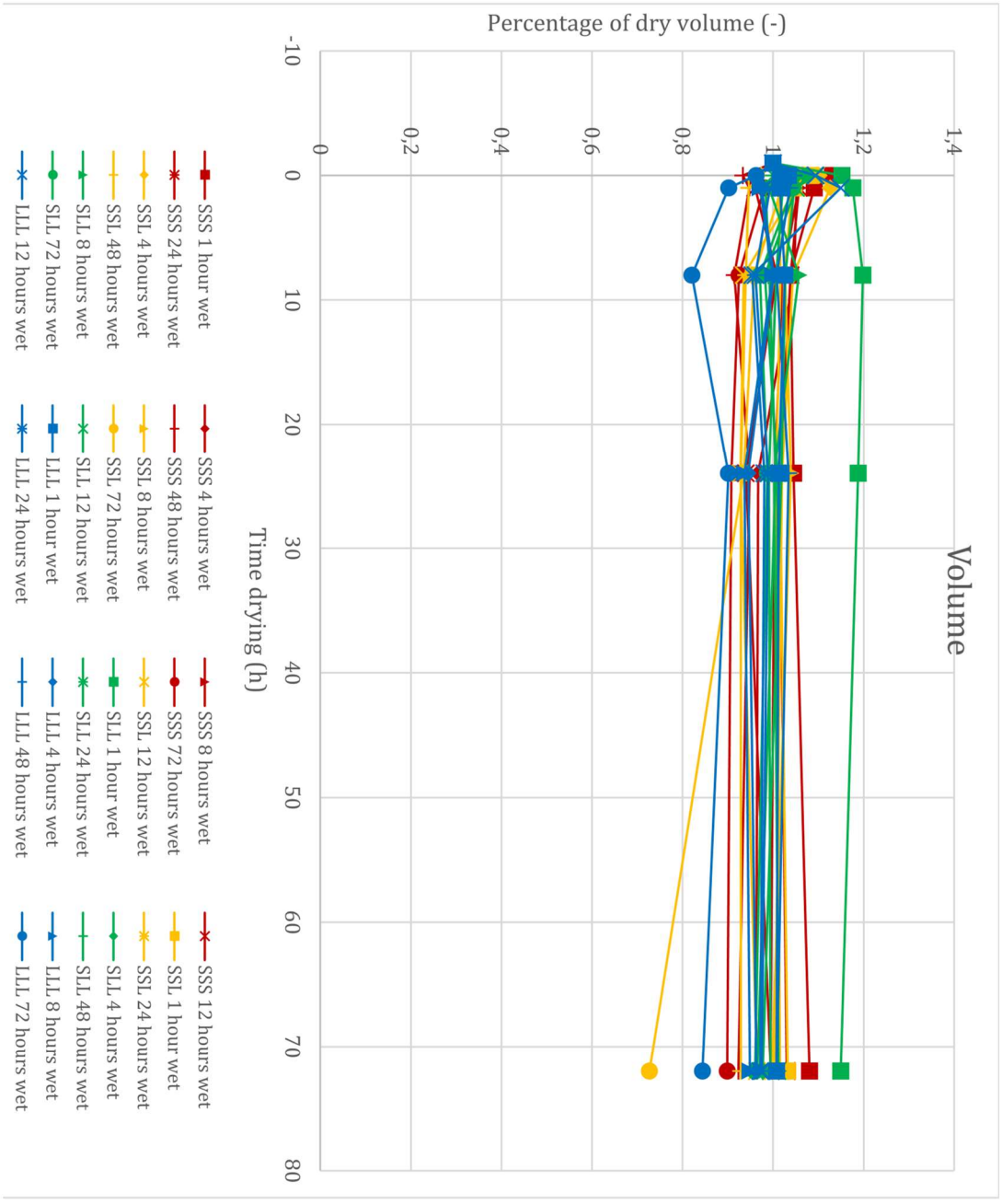

Figure 4.10: *Normalized volume over time drying. The color of the marker indicates how long the specimen was in the water while the shape of the marker indicates the material composition.*

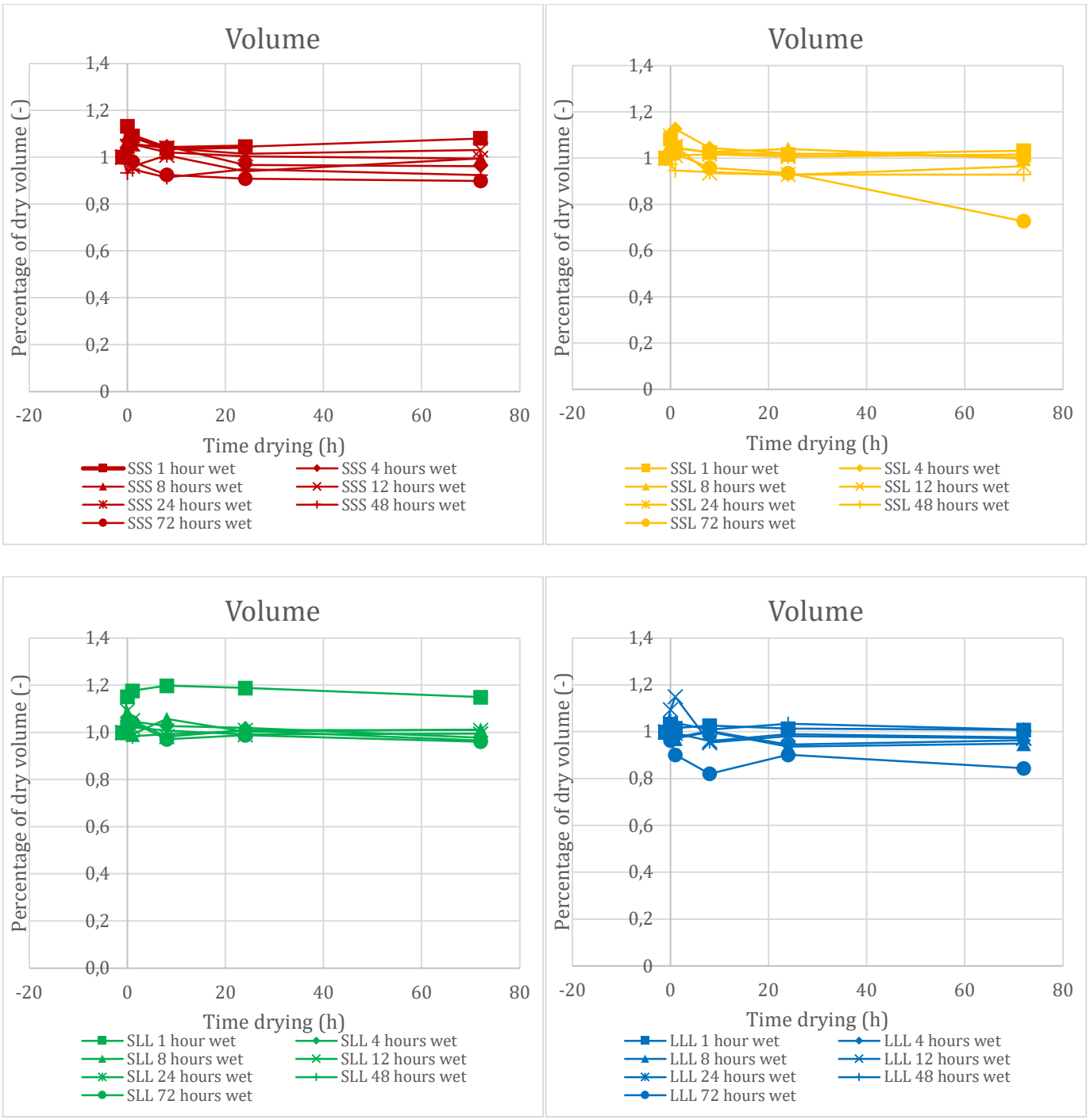

Fig 4.11: *Volume over time separated by material mixture a) SSS b) SSL c) SLL d) LLL*

Compression test: Impact of wetting

The results from compression test: impact of wetting is presented in table 4.3 with figure 4.12 showcasing the maximum stress the material experienced compared with the time it was in water during the aggravated wet-dry experiment. The result differs greatly from compression test: unmodified specimen, with much lower maximum stress and modulus of elasticity.

Table 4.3: Compression test: Impact of wetting

Specimen		Maximum Force [N]	Maximum Stress [N/mm2]	E-modulus [N/mm2]
SSS	Spec SSS0	30.5	0.034	8.979
	Spec SSS1	124.1	0.128	1.076
	Spec SSS2	190.9	0.220	2.447
	Spec SSS3	134.9	0.127	1.092
	Spec SSS4	121.6	0.142	0.977
	Spec SSS5	120.7	0.135	0.837
	Spec SSS6	156.5	0.164	1.142
	Spec SSS7	107.0	0.109	0.611
SSL	Spec SSL0	90.9	0.100	1.233
	Spec SSL1	123.9	0.125	1.767
	Spec SSL2	126.0	0.136	2.027
	Spec SSL3	111.8	0.115	1.360
	Spec SSL4	122.0	0.122	1.219
	Spec SSL5	133.3	0.143	1.609
	Spec SSL6	116.0	0.127	1.654
	Spec SSL7	152.2	0.170	1.714
SLL	Spec SLL0	110.3	0.133	3.029
	Spec SLL1	53.9	0.056	0.789
	Spec SLL2	94.4	0.101	0.794
	Spec SLL3	61.1	0.063	1.141
	Spec SLL4	122.8	0.130	1.639
	Spec SLL5	121.7	0.129	2.049
	Spec SLL6	115.6	0.117	1.288
	Spec SLL7	115.8	0.117	2.173
LLL	Spec LLL0	96.7	0.100	2.592
	Spec LLL1	56.5	0.064	1.380
	Spec LLL2	57.2	0.057	1.092
	Spec LLL3	14.0	0.015	2.66
	Spec LLL4	62.6	0.064	1.405
	Spec LLL5	88.7	0.098	1.875
	Spec LLL6	74.2	0.082	1.700
	Spec LLL7	110.35	0.122	2.010

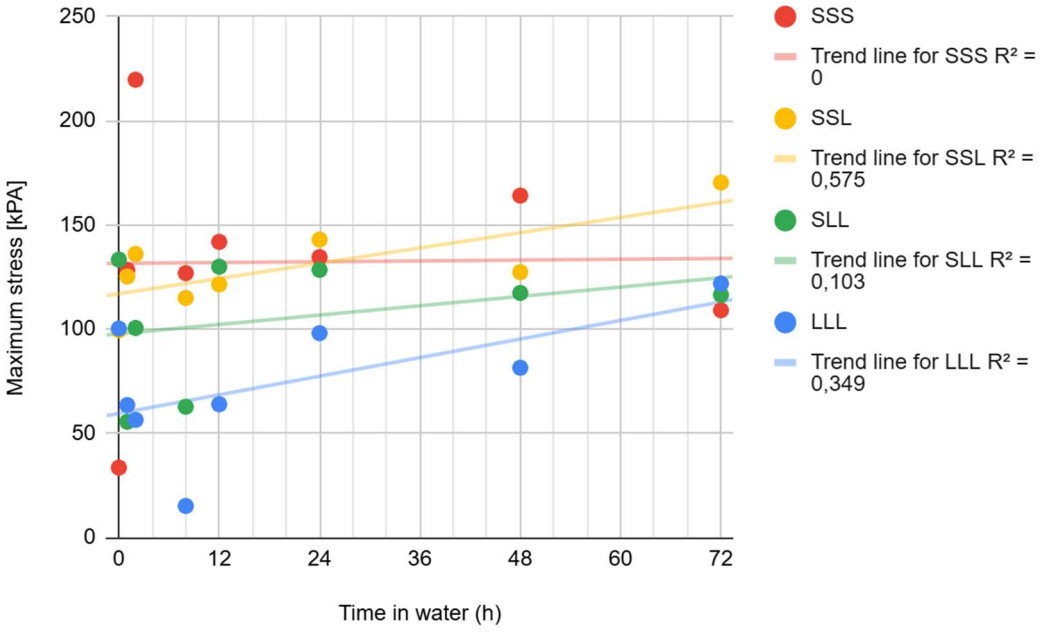

Figure 4.12: *Maximum Stress/Time in water Compressive test: Impact of wetting*

5 Finite-element modelling and calculations

The purpose of the finite element model was to see how forces and stresses flow through the material and to see if the loads from the example building would lead to failure in the material based on the strength data determined in ***chapter 4***.

A finite element model of a cordwood wall or structure was established based on the building designed in Globwood (Stålhammar, O. 2025), including dimensions and load cases. The scope of the model was determined by the exposure test. The model was used to model the behavior with parameters used according to the findings in this project.

5.1 The Globwood Retreat

The thesis work (Stålhammar, O., 2025) included the designing of a new building using the modified cordwood technique. The Globwood Retreat is a combined hiking cabin and sauna (*figure 5.1*). The building consists of three rooms and two covered entrances.

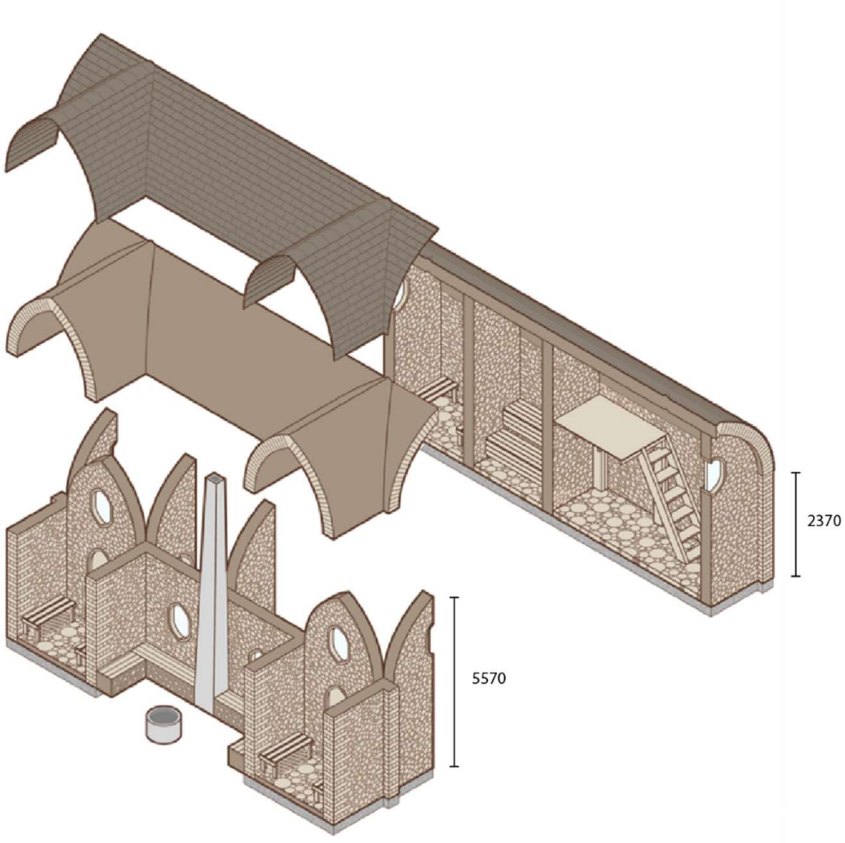

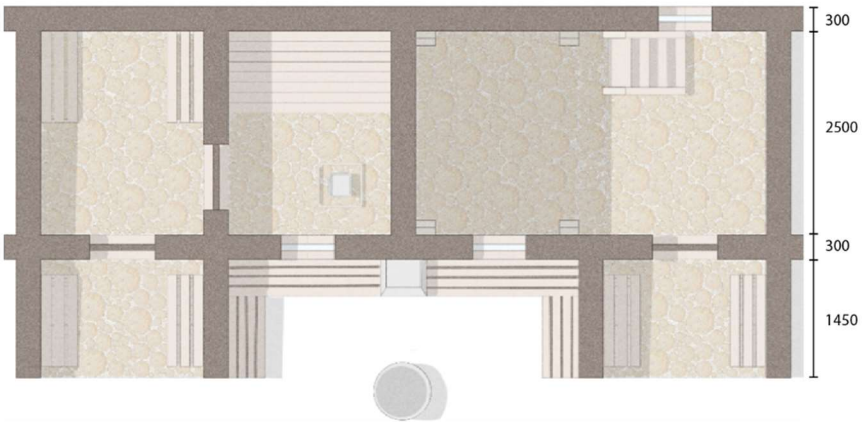

Figure 5.1: *a) Exploded isometry of The Globwood Retreat b) Plan of The Globwood Retreat*

5.2 Loads from the example structure.

The walls are 2.37 m tall and 0.3 m thick. Since the analysis area was 1 m tall the part of the wall that is above that will be analyzed as an external load. Seventy percent of the wall is log-ends and thirty percent is binder which gives an effective density of the wall.

$$\rho_{\text{wall}} = V_{\%pine}\rho_{\text{pine}} + V_{\%binder}\rho_{\text{SLL}} = 435\ kg/m^3 \quad \text{eq. 5}$$

$$V_{\%pine} = 70\ \%\ , V_{\%binder} = 30\ \%$$

$$\rho_{pine} = 450\ kg/m^3$$

$$\rho_{SLL} = 400\ kg/m^3$$

The permanent loads are the self-weight of the wall over the analysis area and the self-weight from the roof with the varying loads being wind load and snow load. See figure 3.4 for geometry.

$$G_k = G_{Wall} + G_{Roof} \quad \text{eq. 6}$$

$$G_{Wall} = \rho_{\text{wall}} * t_{wall} * h_{wall} * l_{wall} * g = 1.752\ kN \quad \text{eq. 7}$$

$$t_{wall} = 0.3\ m\ , h_{wall} = 1.37\ m\ , l_{wall} = 1\ m$$

$$G_{roof} = \rho_{\text{roof}} * V_{roof} * g = 3.219\ kN \quad \text{eq. 8}$$

$$V_{roof} = 0.755\ m^3$$

$$G_k = 4.971\ kN$$

The varying load is the snow load. Snow load is calculated according to the equations from **chapter 2.4.2.**

$$s = \mu_i C_e C_t s_k\ [kN/m^2] \quad \text{eq. 2}$$

For $\beta > 60°$, $\mu_3 = 0$ eq. 3a

For $\beta \leq 60°$, $\mu 3 = min\left[0.2 + \frac{h_{vault}}{w_{vault}}, 2.0\right] = 1.23$ eq.3b

$$h_{vault} = 3.2\ m\ \ , w_{vault} = 3.1\ m$$
$$S_k = s * \frac{ls}{2} * l_{wall} = 2.38\ \text{kN} \qquad \text{eq. 9}$$
$$l_s = 2.58\ m$$

The total external load combination is then:

$$Q_k = \gamma_d(1.2\ G_k + 1.5\ S_k)/k_{mod} = 10.85\ kN \qquad \text{eq.10}$$

or

$$q_d = \frac{Q_k}{\text{A}_{wall}} = 36.2\,\frac{kN}{m^2} = 0.0362\ MPa \qquad \text{eq.11}$$

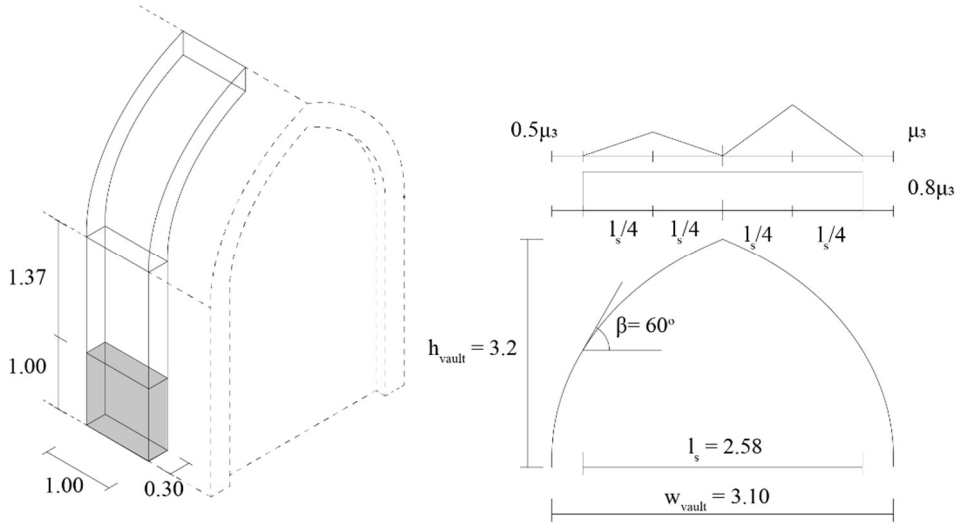

Figure 5.2: *a) Analysis area and b) Snow load form factor*

5.3 ABAQUS model

Geometry

The geometry was a 1 m by 1 m square section of the wall. The geometry was created in Rhinocerous3D and imported into ABAQUS as two elements, log-ends and binder. The section was 71 % log-ends and 29 % binder. Three sizes of log-ends are used to simulate natural variation. The radii are 75 mm, 50 mm and 37.5 mm respectively. See figure 5.3.

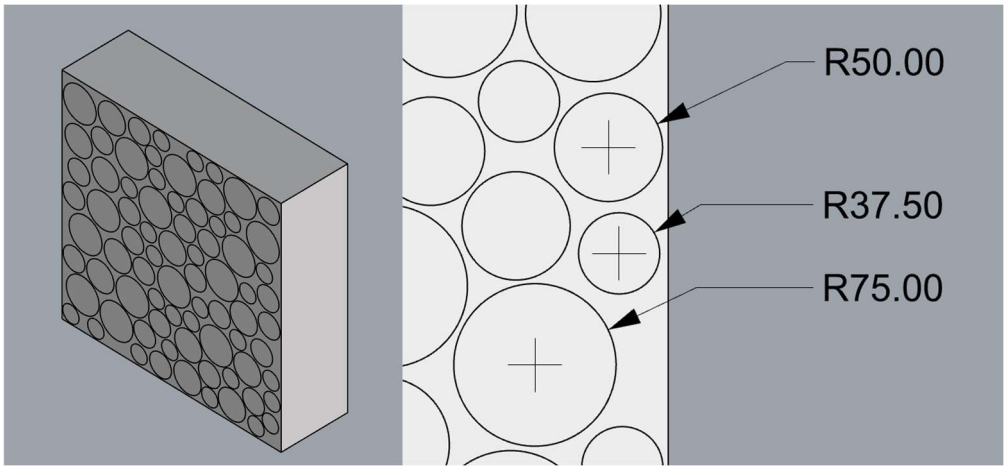

Figure: 5.3: *a) Rhino geometry b) Radii of log-ends*

Properties
The binder was assigned a modulus of elasticity of 8.44 N/mm2 corresponding to the value acquired from the compression test: unmodified specimen. The value used for the E-modulus of the wood was 460 N/mm2 for radial stiffness of pine. The Poisson's ratios used are 0.2 for the binder and 0.16 for the log-ends. The densities used are the same as in chapter 5.2

Mesh settings
The mesh size is determined based on a mesh convergence study. See chapter 5.4. An example mesh is shown in *figure 5.4*.

Boundary conditions
The right and left sides use symmetry boundary conditions, and the bottom is prevented from moving along the Y-axis. The boundary conditions are shown in *figure 5.4 a*.

Interaction
The interaction between the log-ends and binder was defined as ties using ABAQUS built-in function to find connection pairs.

Loads
The wall segment was loaded by self-weight and external loads from the structure specified in chapter 3.4.1.

The external load was applied as a pressure load, q_d, on the top face.

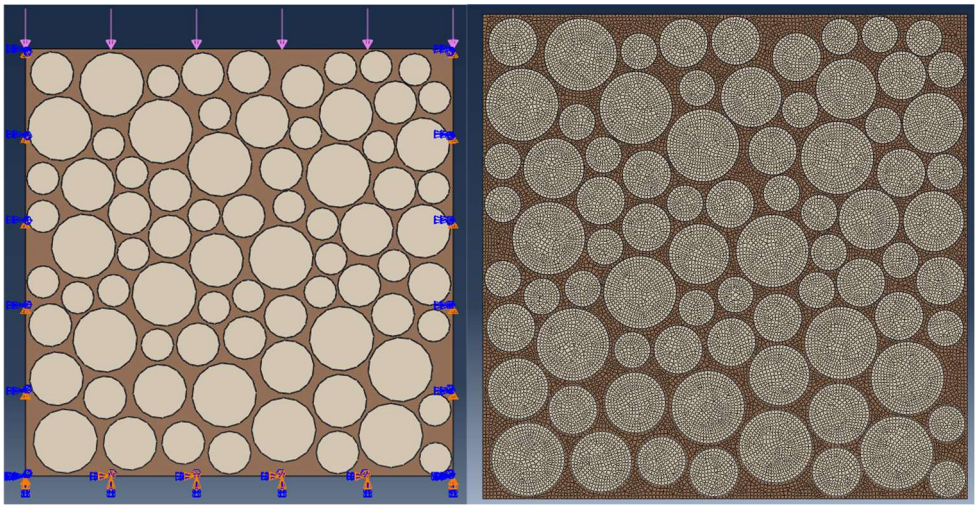

Figure 5.4: *a) Loads and boundary conditions. b) Mesh*

5.4 Mesh convergence

Mesh convergence is determined through increasing the number of elements and measuring the difference in a result parameter, e.g. maximum von Mises stress. A finer mesh results in a more accurate model but increases the computation time. How fine mesh can be used depends on the hardware the simulation is run on. A mesh that is too rough is unable to represent the behavior of the model.

For this mesh convergence an initial mesh size 0.02 m was used with the mesh size halving with each refinement. Von Mises stress were used as the dependent variable. The number of mesh divisions in direction of the thickness of the wall is kept constant.

5.5 Comparison with other binders

The same finite-element model is run with cement and clay binder. The same mesh and boundary conditions are applied as in chapter 5.3 but with a different load q_d, densities and modulus of elasticity.

The density and modulus of elasticity are taken from the table in chapter 1.2.3 and the load q_d is recalculated using the same procedure as in chapter 5.2, the values are presented in table 5.1.

Table 5.1:

Binder	**Modulus of Elasticity [N/mm^2]**	**Density [kg/m^3]**	**q_d [N/mm^2]**
Cement	23000	2200	0.0643
Clay	3950	1924	0.0599

5.6 Calculations based on Eurocode

The purpose of the calculation was to act as a control to the FE-model and to see if the building would be buildable. Additionally, going through the calculation process identified gaps where further studies are needed for the material to be up to code and what parameters are needed to be determined.

In the ultimate limit state the following statement has to be true.

$$N_{Ed} \leq N_{Rd} \qquad \text{eq. 3b}$$

Where N_{Ed} is similar to the external load calculated in chapter 3.2.1 but additionally includes the analysis volume, increasing the load from 10.9 kN to 12.6 kN.

The ultimate compressive resistance is calculated as using the equations in chapter 2.4.1

$$N_{Rd} = \phi_s t f_d l \qquad \text{eq. 8}$$

Where the design strength, f_d, is

$$f_d = f_k/\gamma_M \qquad \text{eq. 5}$$

Taking the partial coefficient, γ_M, to be 2.5 which is the worst-case scenario listed in Eurocode.

And where the strength of the masonry, f_k, is

$$f_k = K {f_b}^{0.7} {f_m}^{0.3} \qquad \text{eq. 2}$$

K is chosen to be 0.2 which similarly is the most conservative value used in Eurocode.

$f_m = 0.39\ MPa$ is the compressive strength measured for SLL in the compression test: unmodified specimen.

$f_b = 7.5\ MPa$ is the compressive strength of pine perpendicular to the fibers

This gives

$$f_k = 0.6179\ \text{N/mm}^2$$

$$f_d = 0.2471\ \text{N/mm}^2$$

With

$$\phi_s = min \begin{cases} 0.85\ \frac{t_b}{t} - 0.0011 \left(\frac{h_{ef}}{t}\right)^2 \\ \left(1.2 - \frac{l_{f,ef}}{l_{ref,c}}\right)\frac{t_b}{t} \geq 0.33 \\ \left(1.2 - \frac{l_{f,ef}}{l_{ref,t}}\right)\left(\frac{t_b}{t}\right)^2 + 0.09\left(\frac{t_b}{t}\right)\left(\frac{h}{t}\right) \geq 0.33 \end{cases} \qquad \text{eq. 9}$$

From the model we have
$h = h_{ef} = 2.37$ m
$t = t_b = 0.3$ m
$l_{f,ef} = 3.1$ m
$l_{ref.c} = 8.0$ m
$l_{ref,t} = 2.8$ m

Which gives us

$$\phi_s = 0.7813$$

And

$N_{Rd} = 57.9$ kN
$N_{Ed} = 12.6$ kN

$U_{Euro} = \frac{N_{Ed}}{N_{Rd}} = 0.22$
Which shows that the material should be strong enough.

6 Results from modelling and calculation

Chapter 6.1. Discusses mesh convergence and the mesh chosen for the model.
Chapter 6.2. Shows the results from the simulations using the lignin binder.
Chapter 6.3. Compare the results from chapter 6.2 with the results from simulations using traditional binders.
Chapter 6.4. Compares the results from the simulations with those achieved from Eurocode calculations

6.1 Mesh convergence

The initial mesh with a mesh size of 0.02 m failed to generate a mesh since parts of the geometry were smaller than the mesh size. A mesh with 0.01 m did generate a mesh and could be refined further to a mesh size of 0.0025 m. The difference in the von Mises stress between a mesh size of 0.005 m and a mesh size 0.0025 m is ~1 % which is good. Further refining the mesh to 0.00125 m resulted in bad elements. The data from the convergence study is presented in table 6.1 with the convergence variable and the number of mesh elements are displayed in figure 6.1.

Table 6.1: *Data to determine mesh convergence, size of elements, number of elements and computation time.*

Mesh_Size [m]	Mesh_num_el_tot [-]	Max von Mises [Pa]	CPU Time [s]	Convergence [-]	Comment
0,02	-	-	-	-	Failed to mesh
0,01	42567	91622	5,9	-	
0,005	158136	99768,6	21	0,0816	
0,0025	601416	101040	84	0,0125	Good
0,00125	-	-	-	-	Bad elements

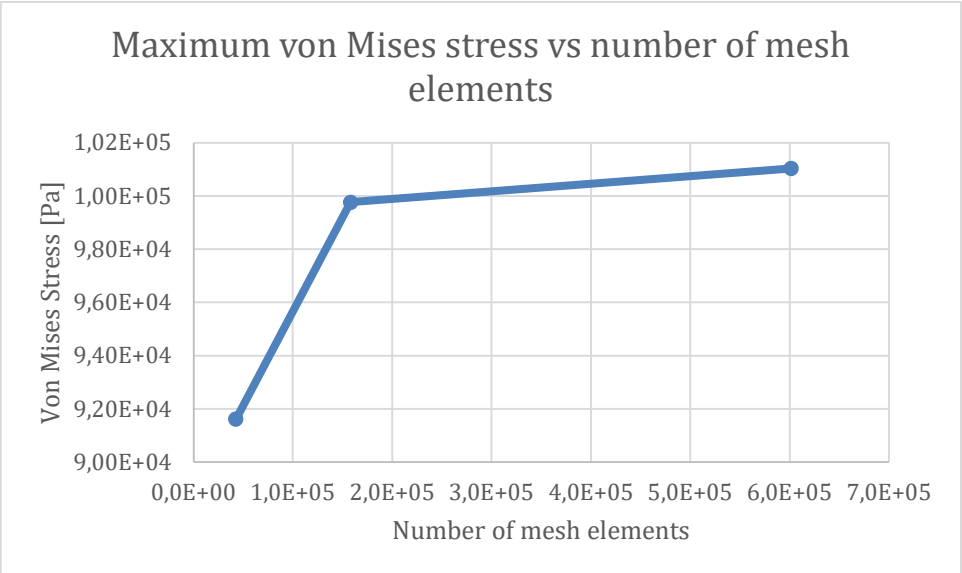

Figure 6.1: *Maximum von Mises stress compared with the number of mesh elements showing convergence*

Figure 6.2 shows the same section of the geometry at different levels of mesh density.

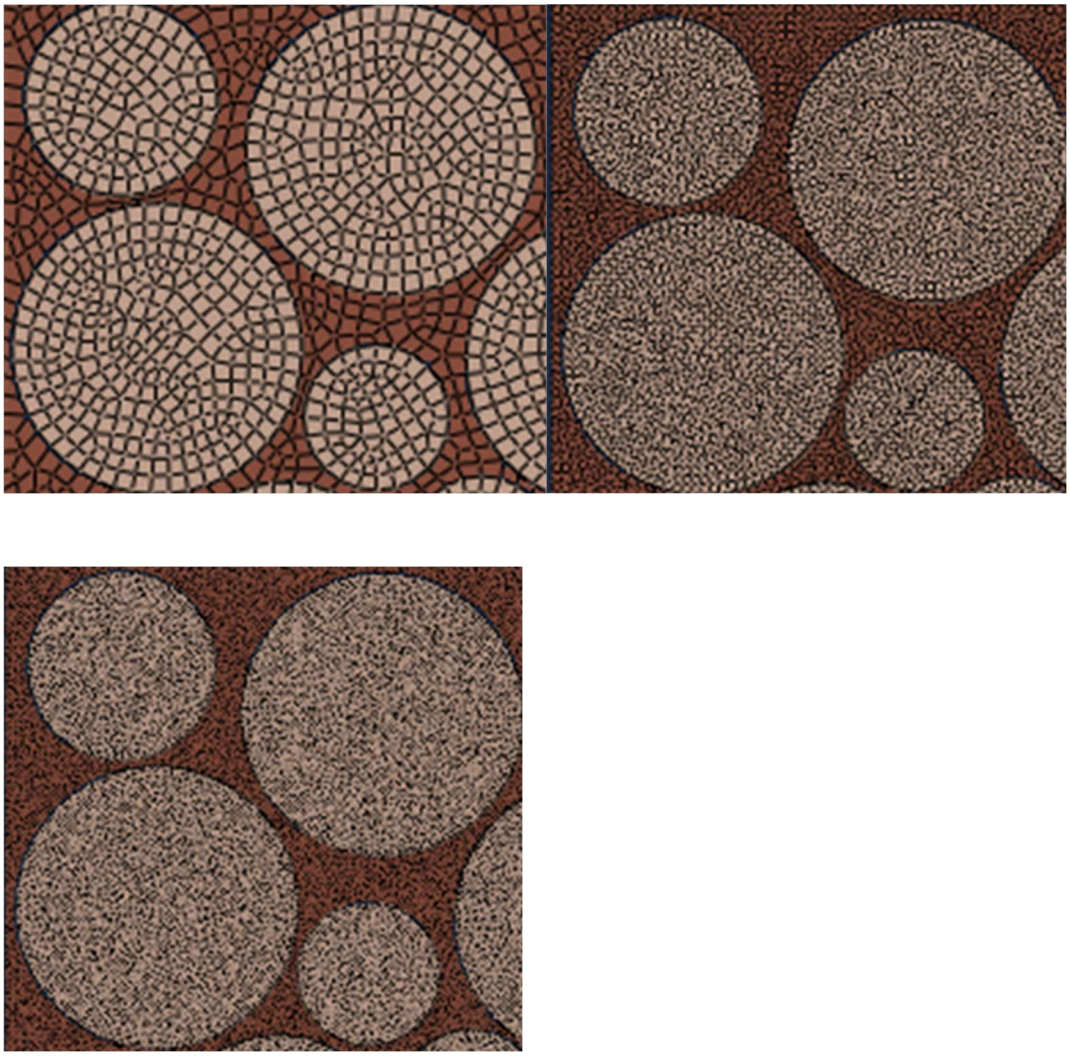

Figure 6.2: *a) 0.01 m mesh b) 0.005 m mesh c) 0.0025 m mesh*

6.2 Compressive stress in Finite-element model

The principal stress is shown in figure 6.3, cooler colors indicate that higher compressive stress and warmer colors indicate tensile stresses.

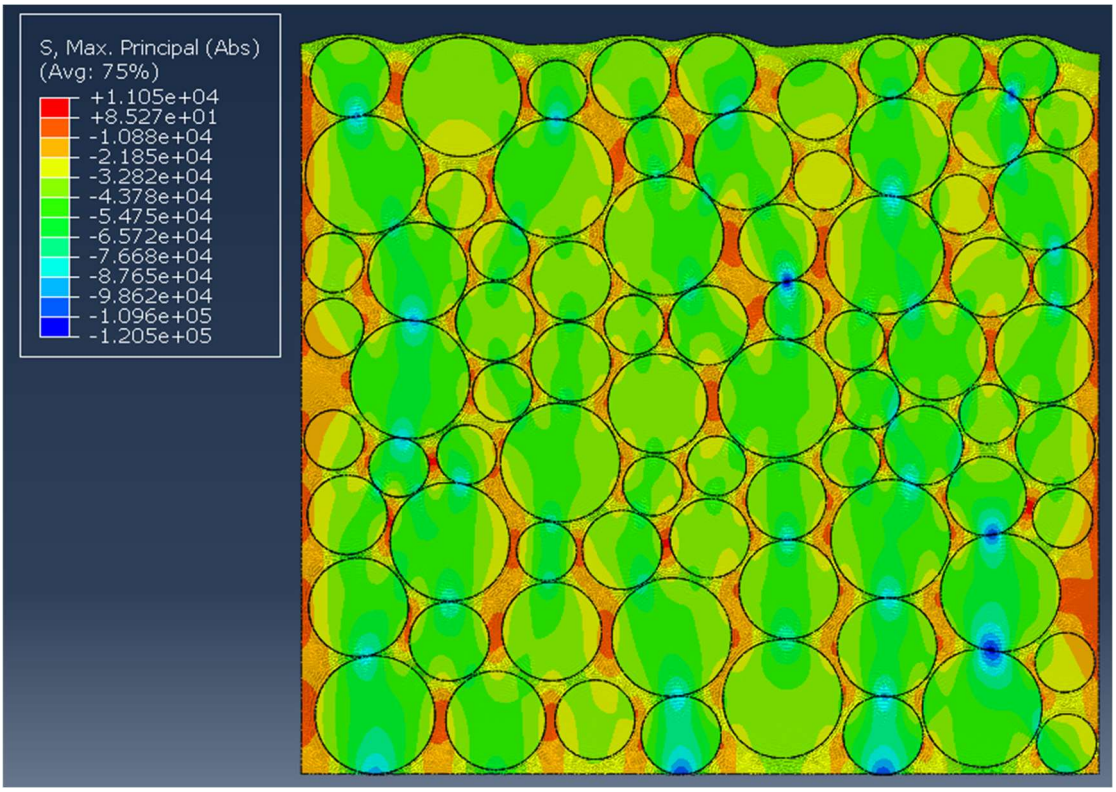

Figure 6.3: *FEA results showing maximum absolute principal stresses of the analysis area using the SLL binder. Red and dark orange show tensile stress; all other colors show compressive stress with the blue areas having the highest compressive stress.*

The maximum compressive stress experienced in the analysis area, $\sigma_{c,MAX}$, is 0.12 N/mm^2. This is less than a third of the measured compressive strength, $f_{c,}$ of 0.39 N/mm^2.

$$U_{FEM} = \frac{\sigma_{c,MAX}}{f_c} = 0.31$$

The force is transferred down through the wall through the stiffer log-ends. But some compressive stress is transferred through the binder since no log-ends are touching each other in the model. The maximum compression is experienced in the binder at the points where the shortest and stiffest load path is from one log-end down to a single other log-end. Where the force can be transferred down from one log-end to two log-ends, instead much lower stress is measured.

The maximum tensile stress experienced is 0.011 N/mm^2, an order of magnitude lower than the compressive stress. The material is likely much weaker in tension compared with compression which means that finding the material's tensile stress becomes an important further area to study.

6.3 Comparison of load paths and stress patterns with traditional binders

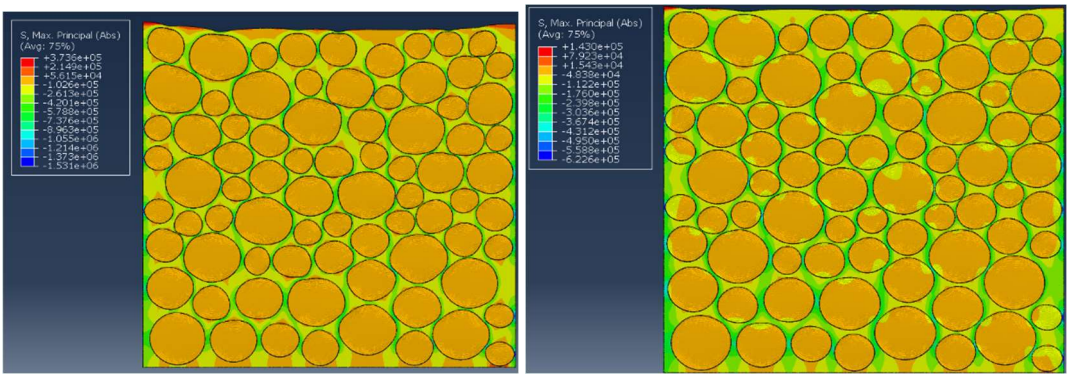

Figure 6.4: *Principal stress for other binders a) Cement b) Clay*

In figure 6.4 the principal stress for the same geometry is shown using cement (left) and clay (right) binders respectively. The load is changed according to the different density as specified in chapter 5.5.

The maximum compressive stress in the cement binder is $\sigma_{c,MAX,cement}$, is 1.53 N/mm^2 which gives a much lower utilization rate than the lignin binder. The transfer of stress is mostly limited to the binder with tensile stresses appearing around the top and bottom of log-ends where the force paths switch direction.

$$U_{FEM,cement} = \frac{\sigma_{c,MAX,cement}}{f_{c,cement}} = 0.06$$

The stress pattern with the clay binder is similar to that of the cement binder but given the lower density of the material the maximum stress is also lower. $\sigma_{c,MAX,clay}$, is 0.62 N/mm^2. However, the utilization rate is higher than for the lignin binder. This stems from the weight to strength ratio of the materials.

$$U_{FEM,clay} = \frac{\sigma_{c,MAX,clay}}{f_{c,clay}} = 0.40$$

Compared with the lignin binder, the stress-patterns are very different for the traditional binders since they have higher stiffness. The stiffness of pine is 460 N/mm2, 50 times higher than the SLL binder. This means that the SLL and SSL binders are the only studied binders with a lower stiffness than the log-ends. Clay, the least stiff of the traditional binder is 500 times stiffer than SLL or 10 times stiffer than wood. Cement is 2000 times stiffer than SLL or 40 times stiffer than the log-ends. How this impacts the structure can be explained with the analogy that a cordwood wall built with cement is similar to a concrete wall with holes in it while a cordwood wall with the lignin binder is more like a stack of firewood with a filler material that close up any holes and keeps the wall together.

6.4 Comparison between Eurocode calculations and finite-element model

There are primarily two aspects that can be compared between the Eurocode calculations and FEM. The first is a control of the validity of the model by comparing the total reaction force at the bottom face of the model with the dimensioning force according to the Eurocode calculation. The total reaction force at the bottom face is 12.14 kN in ABAQUS model, compared with N_{Ed} of 12.6 kN in Eurocode calculation. The difference stems from not multiplying the self-weight of the analysis area (1.28 kN) in ABAQUS with the safety factor = 1.2. Doing so yield 12.4 kN

The second aspect we can compare is the utilization rate we find according to each method. Since both methods analyze and compare the compression strengths of the material these values should be similar. A difference between the values would depend on the constants assumed in the Eurocode calculation.

The utilization rate according to the Eurocode calculation is 0.22 compared with the utilization rate in the FEM is 0.31. The FEM is more likely to be closer to the truth than the Eurocode calculation. This implies that different values of the assumed constants need to be considered for more accurate calculations. Some proposed constants to investigate are α and β in equation 1. These constants assume a normal or lightweight mortar and even lightweight mortars are much stronger, heavier and stiffer than the SLL binder used in this report. Other constants that should be studied are K from the same equation.

Neither method looks at the tensile or bond strength of the composite, since testing for these are outside the scope of this thesis. Implementing these in the FEM would not decrease the utilization rate since the highest utilization rate is used for comparison.

7 Discussion

The discussion in this chapter directly maps back to the research questions in **chapter 1.3.**
Chapter 7.1 answers the question: What is the lignin binder's physical and mechanical properties? How does it compare with traditional binders?
Chapter 7.2 answers the question: Where is the binder suitable to be used within a cordwood structure?
Chapter 7.3 answers the question: Is it possible to design the structure from Stålhammar, O. (2025) to achieve a structural sound building?

7.1 Mechanical properties and comparison with traditional binders

Comparison

Table 5.1: Comparison

Binder Type	E-modulus (MPa)	Compressive strength (MPa)	Density (kg/m3)
Lime-Cement-Sand*	6465	3.02	2069
Cement**	23000	25	2030
Clay***	3950	1.54	1924
SLL	13.7	0.39	450
SSL	7.9	0.40	390

Data from *Soleymani, A., et al. 2022 **Marques, A I., et al. 2020 ***Becker, C., et al. 2024

Table 1.2: *Results from Brics, A., et al (2022)*

Binder Type	Compressive strength (MPa)
Clay	1.94
Lime	7.12
Cement	36.76

Both binder candidates (SLL and SSL) show a low compressive strength and a low modulus of elasticity compared to lime-, cement-, and clay mortar. The compressive strength is less than half of the lowest strength shown by any traditional binders limiting their use to only certain construction elements.

The difference in the results between compression test: unmodified specimen (CT:US) and the control specimen in compression test: impact of wetting (CT:IW) shows that there exists a parameter that affects the strength of the material. The known differences in the test setup are that CT:US uses larger un-sawn specimen while CT:IW use smaller sawn specimen. This would suggest that either the force is able to disperse differently in the larger specimen allowing the material to take more stress before cracking or that the outer layer of the material that is intact in the un-sawn specimen in CT:US and only partially present in the sawn specimen in CT:IW is more important for the materials strength and stiffness. Of these alternative two is consistent with observations of the

material that it is much stiffer in the outer layer and that the inner core is still softer and less cohesive.

Potentially other factors could influence the properties. This could be small changes in the material mixture from variations in the wall-paper paste's water ratio, the soaking time of the paper sludge, or the variation in the saw-dust mixture from the workshop. The difference in drying time since the specimen was created could also be a possible influence. The specimen in CT:IW were created in the spring of 2025 while the specimen in CT:US were created in the fall of 2025. More experiments are necessary to control for these variables and to determine what impacts the material's strength.

From the results of just CT:US we can see that a change in ratio between sawdust and lignin produces a small but noticeable change in material stiffness and strength. The material shows consistent properties within the same material batch. An experiment with a larger number of specimens is needed to calculate how consistent the material is.

With more time and resources, more experiments could be performed, giving higher confidence in the results.

7.2 Suitable use cases

Cordwood with a lignin binder is a weaker material composite compared to cordwood with a traditional binder. The binder is less stiff than the log-ends which makes the behavior different from the traditional alternatives, as seen in **chapter 6.3**. Instead of the compression force mainly being transferred through the binder, the load is transferred through the log-ends with only some specific areas of the binder experiencing compression stress. This means that the wall acts somewhere between dry masonry and mortared masonry. From this it is reasonable to limit the use of this binder to smaller, one-story buildings.

The tensile strength was not investigated in this thesis but from the behavior displayed in the FEM model it will be an important parameter to consider for future experiments.

Vaults are possible with dry masonry but are usually limited in use. Since the log-ends do not have as much contact with each other as rectangular blocks, the vault would likely be weaker. Further studies are necessary to confirm if lignin cordwood masonry is suitable for vaults.

The material is affected by the weather and can degrade over time. In an unprotected environment the binder can degrade quickly depending on the mixture. A recipe containing both lignin and sawdust show much better survivability than a mixture containing only one of them. This durability is further increased with partial coverage of the specimen. For the duration of the experiment the protected specimen showed very little damage. This means that the binder can be used on outside facing elements if care is taken to protect it with a roof. The material should work with no problem in dry indoor environments.

7.3 The Globwood retreat

According to both the Eurocode calculations and the finite-element model, the SLL binder is sufficiently strong for the building designed in Stålhammar, O. (2025). In the

model a 300 mm thick wall was assumed. This thickness was chosen based on dimensions commonly used in cordwood buildings, where that choice usually is motivated by R-values.

Using Eurocode for calculation is not unproblematic with novel building materials. Many calculations are based on lists or tables of known parameters with different constants used for different variations of material combinations.

In the Eurocode sections of this report, many assumptions were made to make the calculations possible. The validity of these assumptions varies with more extensive testing being necessary to verify the results and the procedure. For example, the assumption is **chapter 2.2** that the climate parameter k_{mod}, is the same for this material as for other engineered wood products can be challenged and should be investigated further. But other assumptions are even more difficult to justify. These include classifying wood's masonry class within Eurocode. In this thesis the harshest alternative in the list in Eurocode was chosen. It can be argued since wood is much weaker than all masonry units that are used that it is not harsh enough, but without further full-scale experiments very little can be sure.

The parameters α and β in equation 1 were chosen for the case that to me sounded closest to the use case studied in this thesis which gave equation 2. But none of the cases fit the kind of mortar or mortar joint usually used in cordwood making this choice questionable. This means that for more realistic calculations, α and β need to be determined specifically for cordwood which is outside the scope of this thesis.

7.4 Further development

A low-weight insulating bio-based binder is still an interesting research area that is worth exploring. Both Mouterde, R., et al (2011) and Brics, A., (2022) tried to look at a binder with a reduced carbon footprint even if their candidates were less radical than the binder suggested in this thesis.

Further studies of light-weight binders should consider other binding agents than wallpaper paste, including finding ways to activate the lignin, but these are not part of this thesis.

The most important parameters that were not tested in this thesis are:

- Bond strength, which can be tested through a so-called "Wrench Test".
- Shear strength
- Composite compression test, where the binder is tested together with the masonry units. This requires large testing equipment but would otherwise be similar to the compression test performed in the thesis.
- Thermal conductivity, a discussion of this parameter with theoretical arguments for an approximate magnitude is part of this thesis, but no physical tests were performed. A proposed method for testing this is the so-called "Guarded Heat Test".

An even longer-term study of the behavior of the material in an outdoor environment to see how the material works exposed to snow and freezing. Some preliminary results for this is shown in appendix IV.

8 Conclusion

Cordwood masonry is building technique with great possibilities. An eco-friendly binder is a development that would reinforce cordwood's biggest strength.

This thesis has provided insights into the material properties of a lignin-sawdust binder. The binder was tested for compressive strength and exposed to an outdoor environment for three months.

The tests show that the SLL binder has a low strength, around 0.4 N/mm^2, and low modulus of elasticity around 13.7 N/mm^2, compared with binders used today. While the material is weaker than currently used materials, both a finite element calculation and an ultimate limit state calculation showed the material to be strong enough in compression for a single-story building. A more advanced FEM that can simulate the interaction between the materials, in addition to more testing of bond strength and tensile strength is necessary to validate the result.

It responds poorly to direct exposure to rain but works sufficiently as long as it's protected by a roof. Fully exposed specimens showed noticeable damage within thirty days the *LLL* and *SSS* samples mostly disintegrated after forty days Additional testing of the binder in an accelerated manner showed that water can lead to loss of material but no relationship between time wet and strength could be established after the specimen had dried again.

9 References

Articles

Becker, A., Zeitler, N., Bujotzek, L., Waldmann, D. (2024) Material properties for the shear design of earth masonry under the influence of relative humidity. *Construction and Building Material,* 451. https://doi.org/10.1016/j.conbuildmat.2024.138692

Boquera, L., Olacia, E., Fabiani, C., Pisello, A.L., D'Alessandro, A., Ubertini, F., Cabeza, L. (2021) Thermo-acoustic and mechanical characterization of novel bio-based plasters: The valorisation of lignin as by-product from biomass extraction for green building applications. *Construction and Building Materials,* 278. https://doi.org/10.1016/j.conbuildmat.2021.122373

Brics, A., Serdjuks, D., Gravit, M., Buka-Vaivade, K., Goremikins, V., Vatin, N.I., Podkoritovs, A. (2022) The Behaviour of Load-Carrying Members from Cordwood. *Buildings* 2022, 1702. https://doi.org/10.3390/buildings12101702

Kalami, S., Arefmanesh, M., Master, E. and Nejad, M. (2017), Replacing 100% of phenol in phenolic adhesive formulations with lignin. *J. Appl. Polym. Sci.*, 134, 45124. https://doi.org/10.1002/app.45124

Maria D'Altri, A., de Miranda, S., Castellazzi, G., Sarhosis, V. (2018) A 3D detailed micro-model for the in-plane and out-of-plane numerical analysis of masonry panels. *Computers and Structures,* 206, 18-30. https://doi.org/10.1016/j.compstruc.2018.06.007

Marques, A. I., Morais, J., Morais, P., Veiga, M. do R., Santos, C., Candeias, P., & Ferreira, J. G. (2020). Modulus of elasticity of mortars: Static and dynamic analyses. *Construction and Building Materials*, *232*. https://doi.org/10.1016/j.conbuildmat.2019.117216

Mouterde, R., Morel, J.C., Martinet, V., Sallet, F. (2010) The mechanical performance of cordwood. *Biosystems Engineering* 108 (2011). 237-243. https://doi.org/10.1016/j.biosystemseng.2010.12.006

Roy, R., Flatau, R. (2015) *Continental Cordwood Conference Papers*. New York, Continental Cordwood Conference.

Soleymani, A., Najafgholipour, M. A., & Johari, A. (2022). An experimental study on the mechanical properties of solid clay brick masonry with traditional mortars. *Journal of Building Engineering*, *58*. https://doi.org/10.1016/j.jobe.2022.105057

Szewczyk, J. (2007) Cordwood heritage. *Urban Heritage: Research, Interpretation, Education*, 120 – 128. https://doi.org/10.3856./uh20070925.120-128

Szewczyk, J. (2023) Building with Stovewood in Eastern Europe (c. 1895 – 1965). *Vernacular Architecture*, 54, 51 – 69. https://doi.org/10.1080/03055477.2024.2317735

Thor, L. (2024) *Kubbhus i värmland.* Karlstad, Värmlands Museum.

Tribot, A., Amer, G., Alio, M.A., Baynast, H., Delattre, C., Pons, A., Mathias, J.-D., Callois, J.-M., Vial, C., Michaud, P., Dussap, C.-G. (2019) Wood-lignin: Supply, extraction processes and use as bio-based material. *European Polymer Journal,* 112, 228 – 240. https://doi.org/10.1016/j.eurpolymj.2019.01.007

United Nations Environment Programme (2025). *Global Status Report for Buildings and Construction 2024/2025: Not just another brick in the wall - The solutions exist. Scaling them will build on progress and cut emissions fast.* Paris. https://wedocs.unep.org/20.500.11822/47214

Zhang, T., Cai, G., Liu, S., Puppala, A. (2016) Engineering Properties and Microstructural Characteristics of Foundation Silt Stabilized By Lignin-based Industrial By-product. *KSCE Journal of Civil Engineering,* 20, 2835-2736. https://doi.org/10.1007/s12205-016-1325-4

Books

Flatau, R. C. (2020). *Cordwood construction best practices: A log home building method using renewable resources and time-honored techniques* (Rev. & updated ed.). Cordwood Construction Resources.

Hagman, O. (2013) *Väggar av ved: en bok om kubbhusens historia och möjligheter.* Gothenburg, A-script.

Hagman, O. (2017) *Mura med ved.* Gothenburg, A-script.

Roy, R. (2016) *Cordwood Building: A Comprehensive Guide to the State of the Art – Fully revised Second Edition.* Gabriola Island, New Society Publishers.

Standards

Swedish Standards Institute (2010) SS-EN 1990:2002 *Eurocode – Basis of structural design.* Stockholm, Swedish Standards Institute.

Swedish Standards Institute (2011) SS-EN 1991-1-1:2003 *Eurocode 1 – Actions on structures – Part 1-1: General actions – Densities, self-weight, imposed load for buildings.* Stockholm, Swedish Standards Institute

Swedish Standards Institute (2005) SS-EN 1991-1-3:2003 *Eurocode 1 – Actions on structures – Part 1-3: General actions – Snow loads.* Stockholm, Swedish Standards Institute

Swedish Standards Institute (2008) SS-EN 1991-1-4:2005 *Eurocode 1 – Actions on structures – Part 1-4: General actions – Wind actions.* Stockholm, Swedish Standards Institute

Swedish Standards Institute (2022) SS-EN 1996-1-1:2022 *Eurocode 6 – Design of masonry structures – Part 1-1: General rules for reinforced and unreinforced masonry structures.* Stockholm, Swedish Standards Institute.

Swedish Standards Institute (2024) SS-EN 1996-3:2024 *Eurocode 6 – Design of masonry structures – Part 3: Simplified calculation methods for unreinforced masonry structures.* Stockholm, Swedish Standards Institute.

Webpages

ArchDaily (2014) Arcus Center for Social Justice Leadership / Studio Gang". https://www.archdaily.com/576630/arcus-center-for-social-justice-leadership-studio-gang ISSN 0719-8884 (Accessed: 6 Feb 2026)

Community Cloud Forest Conservation [CCFC] (no date) *Build and Beyond* https://cloudforestconservation.org/our-work/build-and-beyond/ (Accessed: 6 Feb 2026).

SMHI (no date) *Ladda ner väderobersvationer* https://www.smhi.se/data/hitta-data-for-en-plats/ladda-ner-vaderobservationer/airtemperatureMean24h/108320 (Accessed: 6 Feb 2026)

I. Appendix: Photos from medium-term exposure test

2025-06-14

2025-06-21

2025-06-28

2025-07-04

2025-07-10

2025-07-19

2025-07-26

2025-08-02

2025-08-14

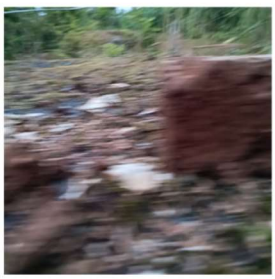

2025-08-21

2025-08-26

2025-09-01

II. Appendix: Aggravated wet-dry experiment

SSS	Before		Immediate after removal from water		After 1 hour drying		After 8 hours of drying		After 24 hours of drying		After 72 hours of drying	
	Dim.	Weight	Dim.	Weight	Dim.	Weight	Dim.	Weight	Dim.	Weight	Dim.	Weight
Control (0 hours wet)	45.14 20.84 20.56	5	-	-	-	-	-	-	-	-	-	-
Spec 1 (1 hour wet)	48.54 20.31 20.16	5	50.01 20.70 21.72	23	49.97 20.30 21.37	21	49.68 20.31 20.45	19	49.13 20.25 20.88	15	49.38 20.62 21.09	7
Spec 2 (4 hours wet)	43.80 20.89 20.68	5	44.14 21.39 21.43	20	43.77 21.30 21.35	19	43.80 21.20 21.33	18	42.23 21.30 20.44	13	42.62 20.54 20.8	6
Spec 3 (8 hours wet)	52.29 21.82 20.50	6	53.11 20.62 22.60	25	53.02 22.65 20.57	23	52.2 20.50 22.32	20	52.32 20.43 21.96	16	52.31 20.74 21.43	7
Spec 4 (12 hours wet)	42.13 20.83 20.60	4	42.73 20.78 21.32	20	43.03 21.80 20.38	18	42.49 20.54 21.51	18	42.07 20.47 21.30	15	42.49 20.67 21,21	5
Spec 5 (24 hours wet)	46.25 20.08 20.14	5	46.53 20.26 20.09	20	45.41 20.24 19.55	20	45.64 20.55 20.11	16	45.45 19.88 19.46	12	46.30 20.53 19.58	5
Spec 6 (48 hours wet)	51.81 20.09 20.29	5	52.74 18.81 19.87	20	52.74 19.16 19.81	20	52.35 18.93 19.49	18	52.39 18.86 20.27	13	5§.84 19.18 19.62	7
Spec 7 (72 hours wet)	49.29 21.37 20.74	5	49.74 22,02 20.63	22	48.83 21.00 20.89	22	47.50 20.52 20.73	19	47.87 20.61 20.10	15	47.07 20.97 19.89	6

SSL	Before		Immediate after removal from water		After 1 hour drying		After 8 hours of drying		After 24 hours of drying		After 72 hours of drying	
	Dim.	Weight	Dim.	Weight	Dim.	Weight	Dim.	Weight	Dim.	Weight	Dim.	Weight
Control (0 hours wet)	50.30 18.77 20.29	6	-	-	-	-	-	-	-	-	-	-
Spec 1 (1 hour wet)	49.70 20.50 19.79	7	50.46 20.70 20.89	21	50.24 20.49 20.48	21	49.96 20.07 20.60	18	49.70 20.72 19.88	15	49.37 20.72 20.34	8
Spec 2 (4 hours wet)	45.02 19.40 20.92	6	46.65 21.27 20.29	19	45.99 20.79 21.42	19	44.45 21.27 20.17	17	44.47 20.92 20.03	15	44.96 20.99 19.43	7
Spec 3 (8 hours wet)	50.24 20.39 19.59	7	50.65 19.92 20.84	22	50.33 20.70 20.06	20	50.71 20.32 19.99	18	50.59 20.34 20.27	15	49.86 20.62 19.48	8
Spec 4 (12 hours wet)	48.92 20.90 20.05	7	49.79 21.68 20.80	21	49.49 20.54 21.21	20	49.08 20.19 19.35	18	48.98 20.39 19.05	12	48.67 20.65 19.67	7
Spec 5 (24 hours wet)	44.80 19.6 20.86	6	46.12 21.30 19.57	19	45.23 21.00 19.50	18	45.07 20.97 19.70	13	46.22 21.12 18.89	12	45.24 20.82 19.75	7
Spec 6 (48 hours wet)	44.55 19.94 20.94	7	45.64 20.99 18.90	19	45.03 20.71 18.88	18	44.86 20.65 18.87	16	44.65 20.75 18.65	11	44.48 20.72 18.75	7
Spec 7 (72 hours wet)	43.95 21.50 19.32	7	44.97 21.08 19.76	19	44.87 21.04 19.71	19	44.64 19.27 20.33	16	44.82 19.95 19.10	13	43.83 20.63 19.02	8

SLL	Before		Immediate after removal from water		After 1 hour drying		After 8 hours of drying		After 24 hours of drying		After 72 hours of drying	
	Dim.	Weight	Dim.	Weight	Dim.	Weight	Dim.	Weight	Dim.	Weight	Dim.	Weight
Control (0 hours wet)	46.31 20.55 19.67	7	-	-	-	-	-	-	-	-	-	-
Spec 1 (1 hour wet)	45.77 20.09 18.74	7	47.30 21.28 19.72	20	46.10 21.15 20.78	20	48.52 20.48 20.78	18	48.53 20.75 20.33	14	48.32 19.68 20.83	9
Spec 2 (4 hours wet)	46.35 18.82 20.24	8	46.68 20.90 18.42	19	46.57 19.08 20.8	19	46.67 20.62 18.84	17	46.48 20.59 18.79	15	46.24 20.59 18.12	8
Spec 3 (8 hours wet)	47.35 18.71 20.22	8	47.84 19.51 20.76	20	47.88 20.39 18.19	19	47.75 20.50 19.34	17	47.59 20.53 18.38	14	47.76 18.53 20.48	8
Spec 4 (12 hours wet)	46.33 20.54 18.36	7	46.98 19.38 20.96	19	46.84 20.92 18.73	18	46.39 20.49 18.05	15	46.80 20.78 18.14	10	46.33 20.74 18.35	7
Spec 5 (24 hours wet)	47.04 18.98 20.29	8	48.25 19.35 19.42	19	48.23 19.98 19.20	19	47.94 20.02 19.00	16	47.83 20.33 18.46	11	47.40 20.10 18.91	8
Spec 6 (48 hours wet)	47.84 20.94 18.62	7	48.23 21.00 18.64	20	48.14 20.77 18.35	19	47.34 18.78 20.81	17	48.30 20.94 18.55	12	47.88 20.62 18.24	7
Spec 7 (72 hours wet)	48.17 20.73 18.97	8	49.73 19.02 20.91	21	49.38 20.82 19.22	20	48.68 18.59 20.32	18	48.72 18.69 20.54	13	47.84 18.63 20.41	8

LLL	Before		Immediate after removal from water		After 1 hour drying		After 8 hours of drying		After 24 hours of drying		After 72 hours of drying	
	Dim.	Weight	Dim.	Weight	Dim.	Weight	Dim.	Weight	Dim.	Weight	Dim.	Weight
Control (0 hours wet)	46.09 20.08 20.74	7	-	-	-	-	-	-	-	-	-	-
Spec 1 (1 hour wet)	46.53 21.03 19.64	8	47.13 21.35 19.74	19	46.59 20.99 19.95	19	47.28 20.90 19.95	16	47.21 20.10 20.51	13	46.43 20.72 20.13	8
Spec 2 (4 hours wet)	49.55 20.72 20.86	9	50.43 20.62 20.89	21	50.05 20.47 20.38	22	50.51 21.39 19.86	20	50.35 20.14 19.96	16	50.63 20.53 19.85	10
Spec 3 (8 hours wet)	44.10 20.50 20.59	7	45.56 20.26 20.49	20	45.36 19.42 20.52	18	45.10 20.66 19.96	16	45.18 20.24 19.07	13	44.86 20.31 19.39	7
Spec 4 (12 hours wet)	46.28 20.79 19.35	8	47,7 20.33 21.01	20	46.30 21.09 20.02	19	46.08 20.59 18.72	17	46.71 20.58 18.99	12	46.27 20.53 19.05	8
Spec 5 (24 hours wet)	47.21 20.72 19.41	9	48.57 19.07 20.92	21	48.08 20.69 18.96	21	48.02 18.50 20.54	18	48.13 18.65 20.92	15	47.53 18.70 20.83	9
Spec 6 (48 hours wet)	47.04 20.26 19.82	9	47.87 20.88 19.76	22	48.14 19.66 20.69	21	47.76 20.42 19.53	20	47.53 20.53 20.02	12	47.00 19.72 20.55	9
Spec 7 (72 hours wet)	47.22 20.76 20.93	8	46.96 20.51 19.14	20	46.82 20.65 19.45	19	46.40 18.66 19.97	17	46.82 20.61 19.17	14	46.15 18.86 19.90	8

III. Appendix: Thermal conductivity

The thermal conductivity of a composite material is dependent on both the components and the structure. Since studying the structure is outside of the scope of this study a simplified approach assumes that the thermal conductivity of wood materials is linearly dependent on the density of the wood product. This approach is used since the binder is made up of wood-based ingredients.

The relationship between wood density and thermal conductivity is roughly linear and is shown in figure III.1. Wood with a density of 800 kg/m3 has a thermal conductivity of 0.18 W/(mK) and wood with a density of 600 kg/m3 is 0.12 W/(mK). In addition, loose sawdust with a density of 80 kg/m3 has a thermal conductivity of 0.07 W/(mK) and dense sawdust with a density of 200 kg/m3 has a thermal conductivity of 0.1 W/(mK).

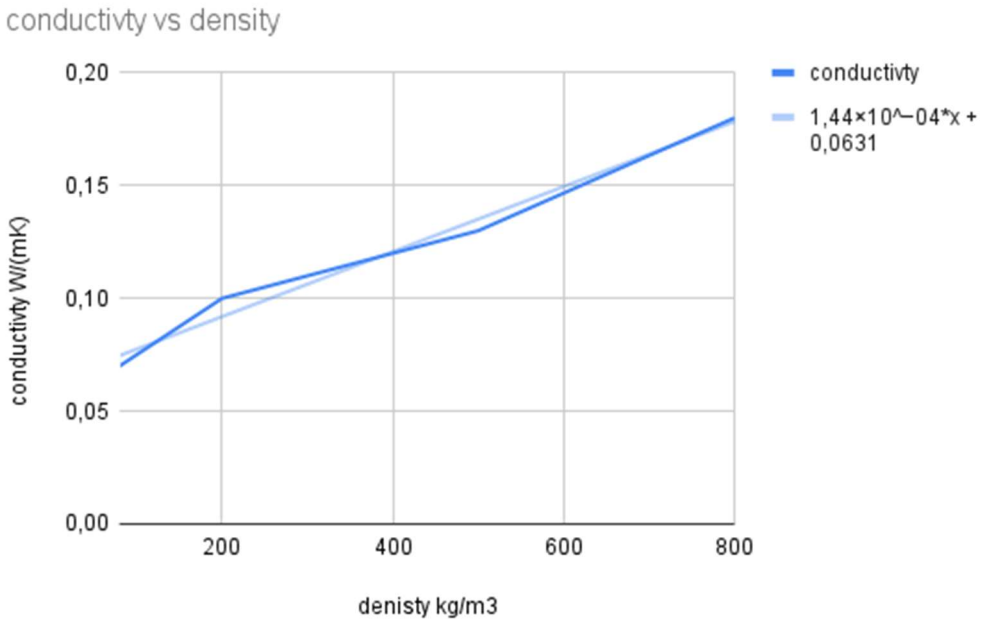

Figure III.1: *Relationship between conductivity and density.*

Interpolating SLL with a density of 400 kg/m3 and SSL with a density of 330 kg/m3 gives values for conductivity 0.12 W/(mK) and 0.11 W/(mK) respectively.

Thermal conductivity, a discussion of this parameter with theoretical arguments for an approximate magnitude is part of this thesis, but no physical tests were performed. A proposed method for testing this is the so-called “Guarded Heat Test”.

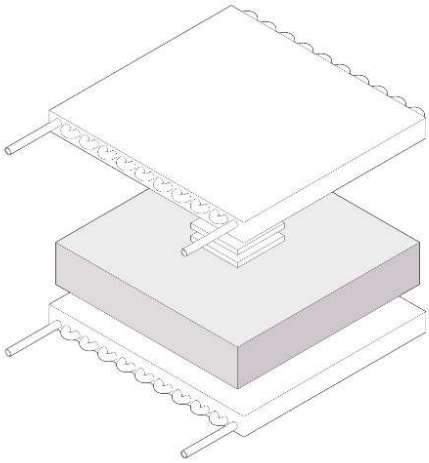

Figure III.2: *Test setup for GHT (Guarded Heat Test)*

IV. Exposure test after winter months

The specimens from the medium-term exposure test were kept in the same environment after the official conclusion of the experiment. Figure IV.1 shows how the specimens in April, 10 months after the experiment began. The unsheltered specimens have suffered additional damage compared to the state they were in at the end of the experiment. The SLL sample still is a recognizable cube, albeit a severely damaged one, the SSL sample on the other hand is no longer in a shape that can be called that. The semi-sheltered specimens have not suffered further than the damage sustained during the experiment, except for the SSS specimen that is a damaged state similar to the unsheltered SSL sample.

Figure IV.1: *Exposure test specimen after 10 months.*

The weather data for the period is presented in figures IV.2 and IV.3.

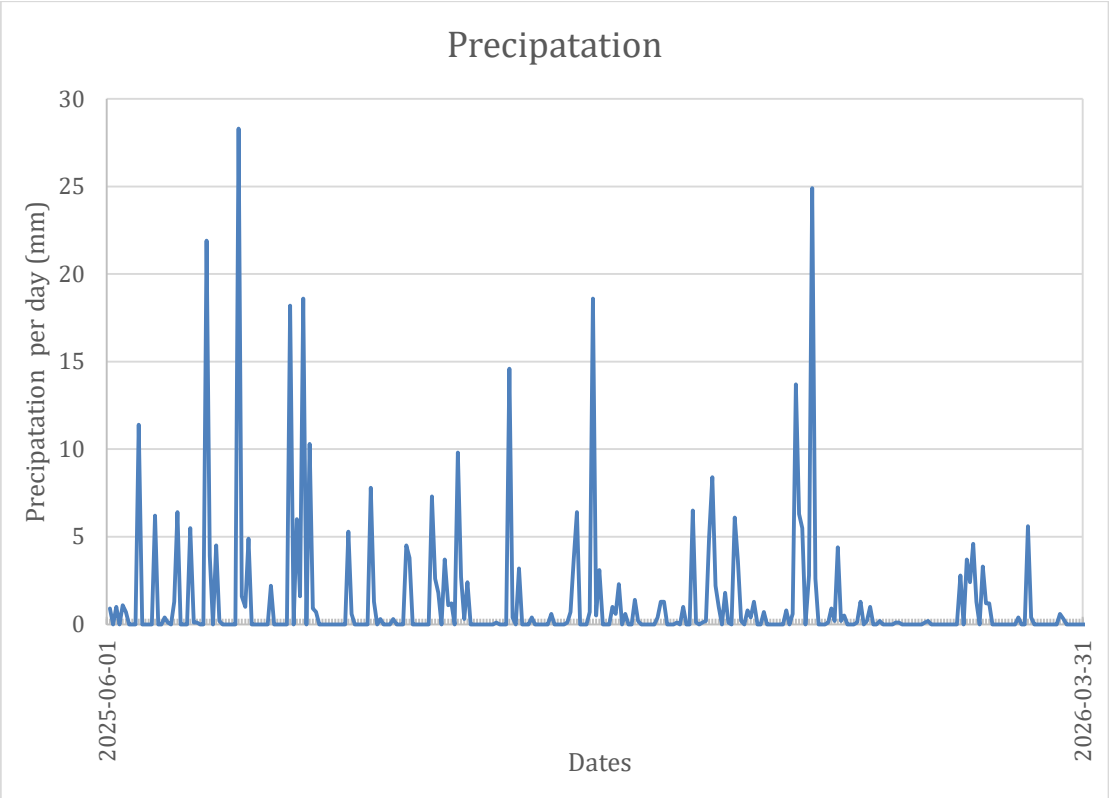

Figure IV.2: *Precipitation between June 2025 and April 2026.*

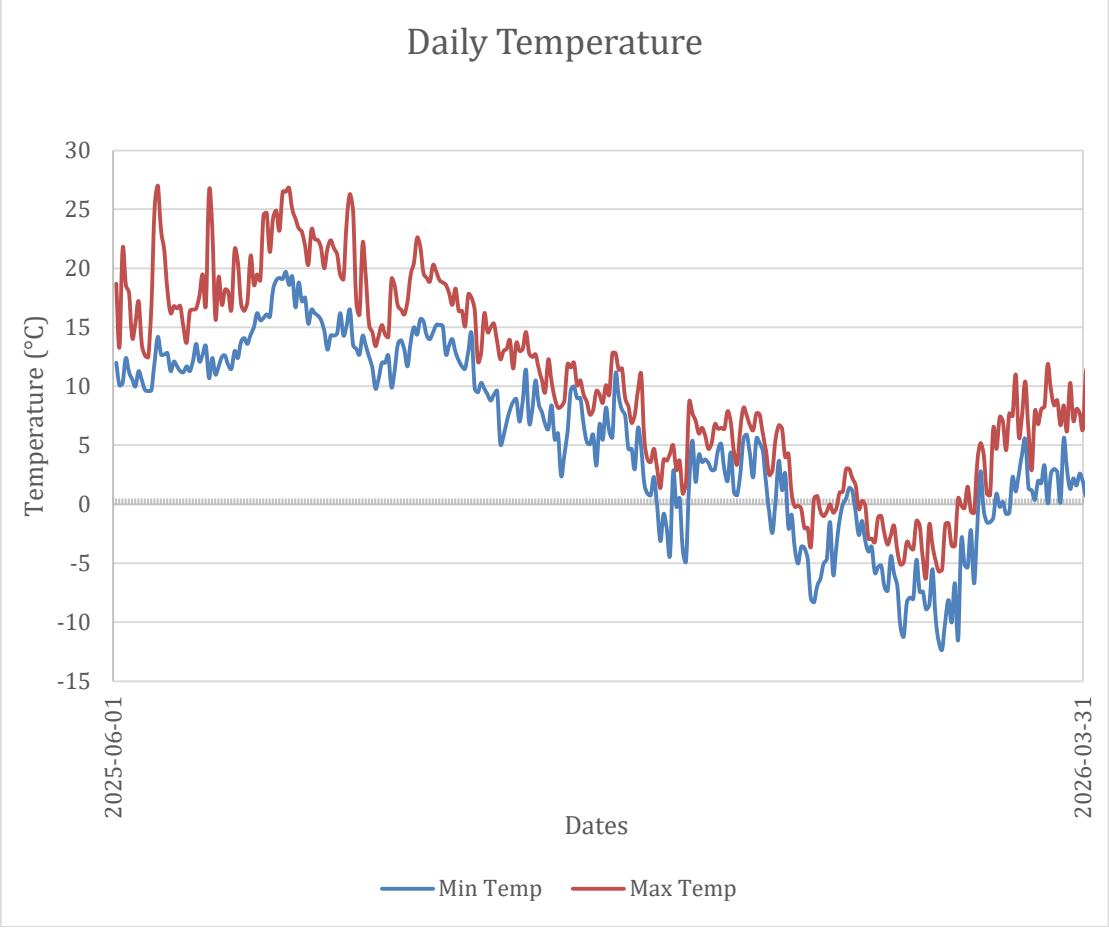

Figure IV.3: *Daily temperature between June 2025 and April 2026.*

DEPARTMENT OF **ARCHITECTURE AND CIVIL ENGINEERING**
CHALMERS UNIVERSITY OF TECHNOLOGY
Gothenburg, Sweden 20xx
www.chalmers.se

CHALMERS
UNIVERSITY OF TECHNOLOGY